

Physiologically Based Pharmacokinetic Modeling of Tacrolimus for Food-Drug and CYP3A Drug-Drug-Gene Interaction Predictions

Supplement S1 - Model Information and Evaluation

Helena Leonie Hanae Loer¹, Denise Feick¹, Simeon Rüdeshcim^{1,2}, Dominik Selzer¹, Matthias Schwab^{2,3,4}, Donato Teutonico⁵, Sebastian Frechen⁶, Maaïke van der Lee⁷, Dirk Jan A. R. Moes⁷, Jesse J. Swen⁷, Thorsten Lehr¹

¹Clinical Pharmacy, Saarland University, Saarbrücken, Germany

²Dr. Margarete Fischer-Bosch-Institute of Clinical Pharmacology, Stuttgart, Germany

³Departments of Clinical Pharmacology, and of Biochemistry and Pharmacy, University of Tübingen, Tübingen, Germany

⁴Cluster of Excellence iFIT (EXC2180) “Image-guided and Functionally Instructed Tumor Therapies”, University of Tübingen, Tübingen, Germany

⁵Translational Medicine & Early Development, Sanofi-Aventis R&D, Chilly-Mazarin, France

⁶Bayer AG, Pharmaceuticals, Research & Development, Systems Pharmacology & Medicine, Leverkusen, Germany

⁷Department of Clinical Pharmacy & Toxicology, Leiden University Medical Center, Leiden, The Netherlands

Funding:

This work is part of the Horizon 2020 INSPIRATION (Qualified Open Systems Pharmacology Modeling Network of Drug-Drug-Gene-Interactions) project. The INSPIRATION project (FKZ 031L0241) is supported by the German Federal Ministry of Education and Research under the framework of ERACoSysMed. Matthias Schwab was supported in parts by the Robert Bosch Stiftung Stuttgart, Germany, and the Deutsche Forschungsgemeinschaft (DFG) under Germany's Excellence Strategy-EXC 2180-390900677.

Conflict of Interest:

Donato Teutonico is an employee of Sanofi. Donato Teutonico uses Open Systems Pharmacology software, tools, or models in his professional role. Donato Teutonico and Thorsten Lehr are members of the Open Systems Pharmacology Management Team. Sebastian Frechen uses Open Systems Pharmacology software, tools, or models in his professional role. Sebastian Frechen is a member of the Open Systems Pharmacology Sounding Board. All other authors declared no competing interests for this work.

Corresponding Author:

Thorsten Lehr, PhD
Clinical Pharmacy
Saarland University
Campus C5 3
66123 Saarbrücken
Germany

Contents

S1 Physiologically Based Pharmacokinetic Model Building	3
S1.1 System-dependent Parameters	3
S1.2 Michaelis-Menten Kinetics	3
S1.3 Clinical Study Data	4
S1.4 Drug-dependent Parameters	6
S2 Physiologically Based Pharmacokinetic Model Evaluation	8
S2.1 Whole Blood Concentration-Time Profiles (Semilogarithmic)	8
S2.1.1 Intravenous Tacrolimus	8
S2.1.2 Immediate-Release Oral Tacrolimus	9
S2.1.3 Extended-Release Oral Tacrolimus	12
S2.2 Whole Blood Concentration-Time Profiles (Linear)	13
S2.2.1 Intravenous Tacrolimus	13
S2.2.2 Immediate-Release Oral Tacrolimus	14
S2.2.3 Extended-Release Oral Tacrolimus	17
S2.3 Urinary Excretion Profiles	17
S2.4 Whole Blood Concentration Goodness-of-Fit Plots	18
S2.5 AUC_{last} and C_{max} Goodness-of-Fit Plots	19
S2.6 MRD of Whole Blood Concentration Predictions	20
S2.7 Predicted and Observed AUC_{last} and C_{max} Values	21
S2.8 Local Sensitivity Analysis	23
S2.8.1 Methods	23
S2.8.2 Results	23
S3 Food-Drug Interaction Modeling	26
S3.1 Clinical Study Data	26
S3.2 Whole Blood Concentration-Time Profiles (Semilogarithmic)	28
S3.3 Whole Blood Concentration-Time Profiles (Linear)	29
S3.4 FDI AUC_{last} and FDI C_{max} Ratio Goodness-of-Fit Plots	30
S3.5 Predicted and Observed FDI AUC_{last} and FDI C_{max} Ratios	31
S4 Drug-Drug(-Gene) Interaction Modeling	32
S4.1 Types of Interactions Implemented	32
S4.1.1 Competitive Inhibition	32
S4.1.2 Mechanism-Based Inactivation	32
S4.1.3 Induction	32
S4.2 Clinical Study Data	33
S4.3 Drug-dependent Parameters DD(G)I Partner	34
S4.3.1 Voriconazole	34
S4.3.2 Itraconazole	35
S4.3.3 Rifampicin	38
S4.4 Whole Blood Concentration-Time Profiles (Semilogarithmic)	40
S4.5 Whole Blood Concentration-Time Profiles (Linear)	41
S4.6 DD(G)I AUC_{last} and DD(G)I C_{max} Ratio Goodness-of-Fit Plots	42
S4.7 Predicted and Observed DD(G)I AUC_{last} and DD(G)I C_{max} Ratios	43
Bibliography	44

S1 Physiologically Based Pharmacokinetic Model Building

S1.1 System-dependent Parameters

Table S1: System-dependent parameters

Enzyme/ Transporter	Reference concentration		Relative organ expression ^c	Localization/ Direction	Half-life liver [h]	Half-life intestine [h]
	Mean ^a [$\mu\text{mol/L}$]	GeoSD ^b				
AADAC	1.0 ^d	1.40 ^e	RT-PCR [1]	intracellular	36	23
CYP2C19	0.76 [2]	1.79 (liver) [3]	RT-PCR [4]	intracellular	26	23
CYP3A4	4.32 [2]	1.18 (liver) [3]	RT-PCR [4]	intracellular	36	23
		1.45 (duodenum) [3]				
CYP3A5	0.04 [2]	2.25 (liver) [3]	RT-PCR [4]	intracellular	36	23
OATP1B1	0.07 ^f [5]	1.54 [5]	RT-PCR [6]	influx	36	23
P-gp	1.41 [7]	1.60 [5]	RT-PCR ^g [6]	efflux	36	23

AADAC: arylacetamide deacetylase, CYP: cytochrome P450, OATP: organic-anion-transporting polypeptide, P-gp: P-glycoprotein, RT-PCR: reverse transcription polymerase chain reaction.

^a: μmol protein/L in the tissue of highest expression

^b: geometric standard deviation of the reference concentration

^c: according to the PK-Sim[®] expression database

^d: if no information was available, the mean reference concentration was set to 1.0 $\mu\text{mol/L}$ and the catalytic rate constant was optimized according to [8]

^e: if no information was available, a moderate variability of 35% coefficient of variation was assumed (1.40 GeoSD)

^f: calculated from transporter per mg membrane protein x 37.0 mg membrane protein per g liver [5]

^g: relative expression in the intestinal mucosa increased by factor 3.57

S1.2 Michaelis-Menten Kinetics

$$v = \frac{v_{max} \cdot [S]}{K_M + [S]} = \frac{k_{cat} \cdot [E] \cdot [S]}{K_M + [S]} \quad (\text{S1})$$

where v = reaction velocity, v_{max} = maximum reaction velocity, $[S]$ = free substrate concentration, K_M = Michaelis-Menten constant, k_{cat} = catalytic rate constant, and $[E]$ = enzyme concentration.

S1.3 Clinical Study Data

Table S2: Clinical studies of tacrolimus used for PBPK model development

Tacrolimus dosing regimen		n	Females [%]	Ethnicity ^a	Frequency ^a of <i>CYP3A5*1</i> [%]	Age [years]	Weight [kg]	Height [cm]	Dataset	Reference
Route	Dose [mg]									
iv (inf, 4 h, SD)	0.015/kg	12	33	Black American	60.5	32.2±10.8	-	-	test	Mancinelli 2001 [9]
iv (inf, 4 h, SD)	0.015/kg	12	42	White American	7.8	44.6±19.1	-	-	test	Mancinelli 2001 [9]
iv (inf, 4 h, SD)	0.015/kg	12	50	Mexican American	20.2	35.7±11.6	-	-	test	Mancinelli 2001 [9]
iv (inf, 4 h, SD)	0.025/kg	8	25	White American	7.8	28±10 (20–50)	78.1±12.9 (67.6–105)	-	training	Bekersky 2001 [10]
iv (inf, 4 h, SD)	0.025/kg	1	0	White American	0	-	-	-	test	Floren 1997 [11]
po (IR cap, SD)	0.5	36	0	Asian	25.8	26.8±5.75 (19–36)	60.77±7.51 (50.0–77.6)	167.24±4.72 (158.5–180.0)	training	Mathew 2011 [12]
po (IR cap, SD)	2	47	0	Asian	25.8	(19–30)	70.0±6.77	-	training	Kim 2017 [13]
po (IR cap, SD)	2	24	0	White American	7.8	37.6	-	-	test	Wring 2019 [14]
po (IR cap, SD)	2	19	11	Japanese	25.8	(22–47)	(50–90)	-	test	Itagaki 2004 [15]
po (IR cap, SD)	3	18	0	White American	7.8	29±7.0 (20–44)	78.6±10.0 (56–90)	178±7.4 (168–188)	training	Bekersky 1999 [16]
po (IR cap, SD)	3	32	34	White American	7.8	38±13.4	76.1±12.0	-	test	Bekersky 1998 [17]
po (IR cap, SD)	3.5	36	50	White American	7.8	25.8 (20–40)	69.8 (47.5–92.4)	173.5 (156.0–195.0)	test	Sansone-Parsons 2007 [18]
po (IR cap, SD)	5	12	58	White American	0	23.5±3.5	66.5±13.5	-	training	Zheng 2012 [19]
po (IR cap, SD)	5	109	0	Asian	25.8	27.8±6.13 (18–44)	61.30±7.44 (46.8–83.0)	167.64±5.51 (153.5–180.0)	training	Mathew 2011 [12]
po (IR cap, SD)	5	8	25	White American	7.8	28±10 (20–50)	78.1±12.9 (67.6–105)	-	training	Bekersky 2001 [10]
po (IR cap, SD)	5	32	34	White American	7.8	31±11 (19–53)	74±11.1 (54.9–94.5)	174.5±8 (159–189)	test	Bekersky 1999 [20]
po (IR cap, SD)	5	12	33	Black American	60.5	32.2±10.8	-	-	test	Mancinelli 2001 [9]
po (IR cap, SD)	5	12	42	White American	7.8	44.6±19.1	-	-	test	Mancinelli 2001 [9]
po (IR cap, SD)	5	12	50	Mexican American	20.2	35.7±11.6	-	-	test	Mancinelli 2001 [9]
po (IR cap, SD)	5	41	81	White American	7.8	47±13 (21–66)	68.0±8.3 (53.1–85.5)	164.8±7.4 (151.5–180.5)	test	Lainesse 2008 [21]

-: not given, ^a: implemented, cap: capsule, CYP: cytochrome P450, d: dosage period in days, ER: extended-release, inf: infusion, IR: immediate-release, iv: intravenous, MD: multiple dose (once daily), n: number of participants, po: oral, SD: single dose; values for age, weight and height are shown as mean ± standard deviation (range).

Table S2: Clinical studies of tacrolimus used for PBPK model development (*continued*)

Tacrolimus dosing regimen		n	Females [%]	Ethnicity ^a	Frequency ^a of <i>CYP3A5*1</i> [%]	Age [years]	Weight [kg]	Height [cm]	Dataset	Reference
Route	Dose [mg]									
po (IR cap, SD)	5	32	34	White American	7.8	31±11 (19–53)	74±11.1 (54.9–94.5)	174.5±8 (159–189)	test	Bekersky 1999 [20]
po (IR cap, SD)	5	15	0	White American	7.8	32.6±10.1 (20–45)	85.2±9.42 (70.9–102)	179±5.77 (170–190)	test	Bekersky 2001 [22]
po (IR cap, SD)	5	24	38	White American	7.8	35±11.4	75.2±14.5	-	test	Groll 2017 [23]
po (IR cap, SD)	5	36	50	European	7.8	27±8.3	72±13	175±9	test	Huppertz 2021 [24]
po (IR cap, SD)	5	36	0	White American	7.8	26±6 (20–49)	75.5±10.4 (52.7–100.1)	-	test	Dowell 2007 [25]
po (IR cap, SD)	5	16	0	White American	7.8	34.0±9.23 (22–45)	82.5±10.3 (64.1–100)	183±6.48 (173–193)	test	Bekersky 2001 [26]
po (IR cap, SD)	5	25	44	White American	7.8	-	-	-	test	Alloway 2020 [27]
po (IR cap, SD)	7	18	0	White American	7.8	29±7.0 (20–44)	78.6±10.0 (56–90)	178±7.4 (168–188)	training	Bekersky 1999 [16]
po (IR cap, SD)	7	18	67	European	7.8	39±16	-	-	test	Stift 2014 [28]
po (IR cap, SD)	8	1	0	White American	0	-	-	-	test	Floren 1997 [11]
po (IR cap, SD)	10	18	0	White American	7.8	29±7.0 (20–44)	78.6±10.0 (56–90)	178±7.4 (168–188)	training	Bekersky 1999 [16]
po (IR cap, SD)	10	27	0	European	7.8	31.4±8.6 (18–46)	71.4±8.0 (57–91)	-	test	Tortorici 2013 [29]
po (ER cap, SD)	2	21	0	White American	7.8	-	86.6	-	training	Mercuri 2016 [30]
po (ER cap, SD)	3	16	0	European	15.6	(18–28)	-	-	test	Vanhove 2019 [31]
po (ER cap, MD, 10d)	5	93	0	European	7.8	-	-	-	training	Gantar 2020 [32]
po (ER cap, SD)	5	113	-	European	7.8	-	-	-	test	Gantar 2020 [32]
po (ER cap, SD)	10	20	0	European	7.8	34 (20–54)	75.2 (53.5–96.9)	-	test	Undre 2017 [33]

-: not given, ^a: implemented, cap: capsule, CYP: cytochrome P450, d: dosage period in days, ER: extended-release, inf: infusion, IR: immediate-release, iv: intravenous, MD: multiple dose (once daily), n: number of participants, po: oral, SD: single dose; values for age, weight and height are shown as mean ± standard deviation (range).

S1.4 Drug-dependent Parameters

Table S3: Drug-dependent parameters of the final tacrolimus PBPK model

Parameter	Unit	Value	Source	Literature	Reference	Description
Tacrolimus						
Molecular weight	g/mol	804.03	Lit.	804.03	[36]	Molecular weight
pKa, acid		9.96	Lit.	9.96	[36]	Acid dissociation constant
Solubility (pH)	mg/mL	0.01 (7.4)	Lit.	0.01 (7.4)	[36]	Solubility
Lipophilicity	log units	5.37	Opt.	2.74–5.594	[36–38]	Lipophilicity
f_u	%	1.2	Lit.	1.2	[39]	Fraction unbound
CYP3A4 $K_M \rightarrow$ sink	$\mu\text{mol/L}$	0.21	Lit.	0.21^a , 1.5	[40, 41]	Michaelis-Menten constant
CYP3A4 $k_{\text{cat}} \rightarrow$ sink	1/min	4.42	Opt.	0.72, 8.0	[40, 41]	Catalytic rate constant
CYP3A5 $K_M \rightarrow$ sink	$\mu\text{mol/L}$	0.21	Lit.	0.21^a , 1.4	[40, 41]	Michaelis-Menten constant
CYP3A5 NM (100%) $k_{\text{cat}} \rightarrow$ sink	1/min	47.30	Opt.	1.1, 17.0	[40, 41]	Catalytic rate constant
CYP3A5 PM (0%) $k_{\text{cat}} \rightarrow$ sink	1/min	0	Calc.	-	-	Catalytic rate constant
GFR fraction		1^b	Asm.	-	-	Filtered drug in the urine
EHC continuous fraction		1	Asm.	-	-	Bile fraction continuously released
Intestinal permeability IR Tac fasted	cm/s	$3.42 \cdot 10^{-6}$	Opt.	-	-	Transcellular intestinal permeability
Intestinal permeability IR Tac fed	cm/s	$3.79 \cdot 10^{-7}$	Opt.	-	-	Transcellular intestinal permeability
Intestinal permeability ER Tac fasted	cm/s	$1.91 \cdot 10^{-6}$	Opt.	$6.58 \cdot 10^{-6}$	[30]	Transcellular intestinal permeability
Cellular permeability	cm/min	0.02	Calc.	Charge dependent Schmitt	[42]	Permeability into the cellular space
Partition coefficients			Calc.	Berezhtkovskiy	[43]	Organ-plasma partition coefficients
Dissolution time (Weibull) IR Tac fasted	min	18.85	Lit.	18.85^c	[44]	Dissolution time (50%)
Dissolution shape (Weibull) IR Tac fasted		0.08	Opt.	0.12^c	[44]	Dissolution shape
Dissolution time (Weibull) IR Tac fed	min	63.03	Opt.	-	-	Dissolution time (50%)
Dissolution shape (Weibull) IR Tac fed		0.94	Opt.	-	-	Dissolution shape
Dissolution time (Weibull) ER Tac fasted	h	3.40	Lit.	3.13^c	[30]	Dissolution time (50%)
Dissolution shape (Weibull) ER Tac fasted		0.06	Opt.	0.12^c	[30]	Dissolution shape
CYP3A4 K_i	$\mu\text{mol/L}$	0.04	Lit.	0.04^a	[45]	Diss. const. inhibitor-enzyme complex (CI)
CYP3A4 K_I	$\mu\text{mol/L}$	2.66	Lit.	2.66	[45]	Conc. for half-maximal inactivation (MBI)
CYP3A4 k_{inact}	1/min	0.30	Lit.	0.30	[45]	Maximum inactivation rate constant (MBI)
CYP3A5 K_I	$\mu\text{mol/L}$	2.69	Lit.	2.69	[45]	Conc. for half-maximal inactivation (MBI)
CYP3A5 k_{inact}	1/min	0.21	Lit.	0.21	[45]	Maximum inactivation rate constant (MBI)

–: not available, ^a: *in vitro* values corrected for binding in the assay ($f_{u,\text{mic}}$) calculated according to [34], ^b: a GFR fraction of 1 corresponds to passive glomerular filtration of a compound, ^c: obtained from literature dissolution profile according to [35], asm.: assumed, calc.: calculated, CI: competitive inhibition, conc.: concentration, const.: constant, CYP: cytochrome P450, EHC: enterohepatic circulation, diss.: dissociation, ER: extended-release, GFR: glomerular filtration rate, IR: immediate-release, lit.: literature, MBI: mechanism-based inactivation, NM: normal metabolizer, opt.: optimized, PM: poor metabolizer, Tac: tacrolimus.

Table S4: Key modeling assumptions, including the resulting modeling decisions

Assumption	Modeling Decision
The liberation of IR and ER tacrolimus can be described using Weibull functions.	Different Weibull functions were implemented for IR and ER tacrolimus.
The excipients contained in IR and ER tacrolimus capsules may affect intestinal permeability differently.	A slightly higher intestinal permeability was incorporated for IR tacrolimus than for ER tacrolimus.
CYP3A4 and CYP3A5 are predominantly involved in the metabolism of tacrolimus.	CYP3A4 and CYP3A5 were incorporated as metabolizing enzymes.
The functional <i>CYP3A5</i> *1 allele and the nonfunctional *3 allele exhibit 100% and 0% activity, respectively.	The reported fraction of functional *1 allele in a study population was used for activity assignment relative to homozygous carriers of the *1 allele. Different levels of activity were implemented by activity-specific CYP3A5 k_{cat} values, i.e., 100% relative activity corresponded to a k_{cat} of 100%.
Frequencies of *1 alleles reported for different ethnic groups are representative for frequencies in the study populations.	In the absence of genotype/phenotype information of a study group, CYP3A5 activity was assumed according to the frequency of the *1 allele observed in the respective ethnic group.
Renal excretion of tacrolimus occurs via passive glomerular filtration.	In PK-Sim [®] , a GFR fraction of 1 was implemented for tacrolimus.
Under fed conditions, the release kinetics differ from those under fasted conditions, e.g., due to altered gastric pH.	Different Weibull functions were implemented for fasted and fed conditions.
Under fed conditions, the absorption of tacrolimus is altered, presumably due to the binding of tacrolimus to lipoproteins and food components, given its pronounced lipophilicity.	A lower intestinal permeability was incorporated for fed conditions compared to fasted conditions.

CYP: cytochrome P450, ER: extended-release, GFR: glomerular filtration rate, IR: immediate-release, k_{cat} : catalytic rate constant.

S2 Physiologically Based Pharmacokinetic Model Evaluation

S2.1 Whole Blood Concentration-Time Profiles (Semilogarithmic)

S2.1.1 Intravenous Tacrolimus

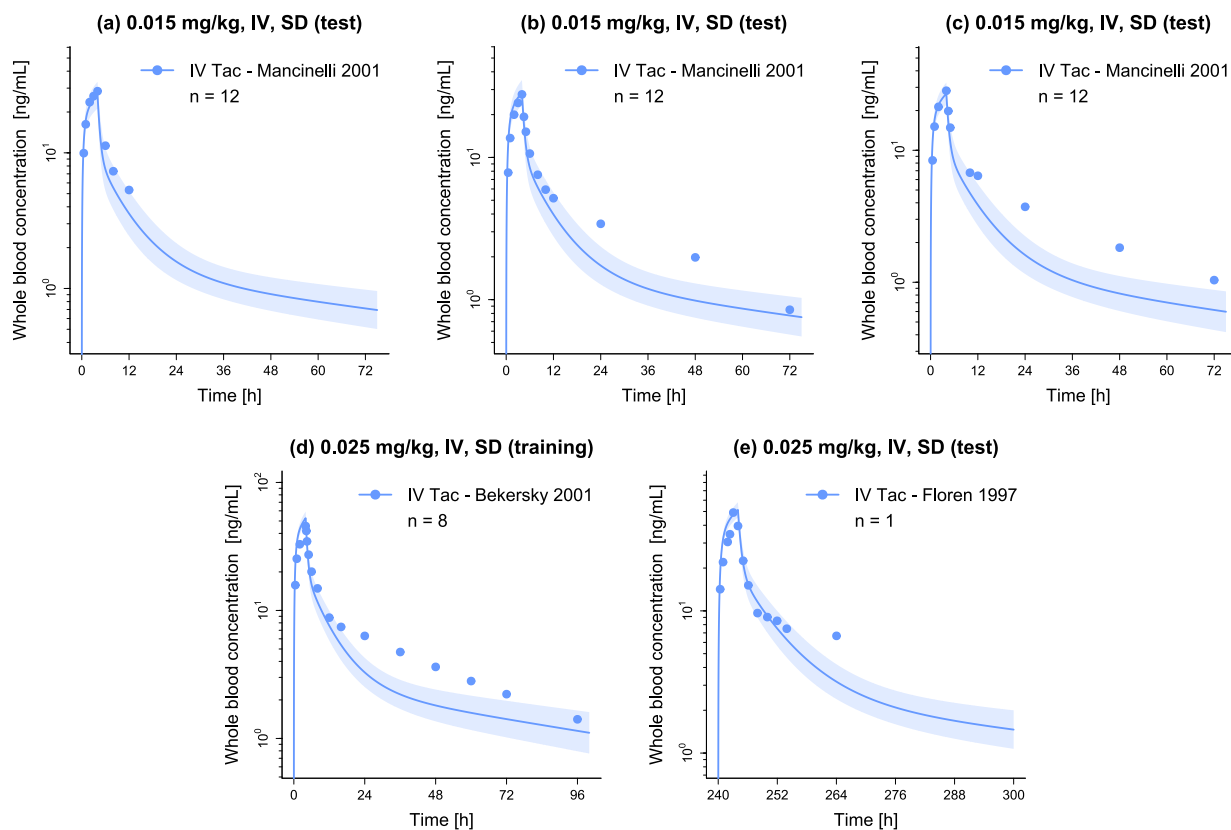


Figure S1: Semilogarithmic plots of predicted whole blood concentration-time profiles of IV tacrolimus (fasted). Solid lines and ribbons represent population predictions ($n = 1000$; geometric mean and geometric standard deviation), while corresponding observed data are shown as dots [9–11]. IV: intravenous, n: number of participants, SD: single dose, Tac: tacrolimus.

S2.1.2 Immediate-Release Oral Tacrolimus

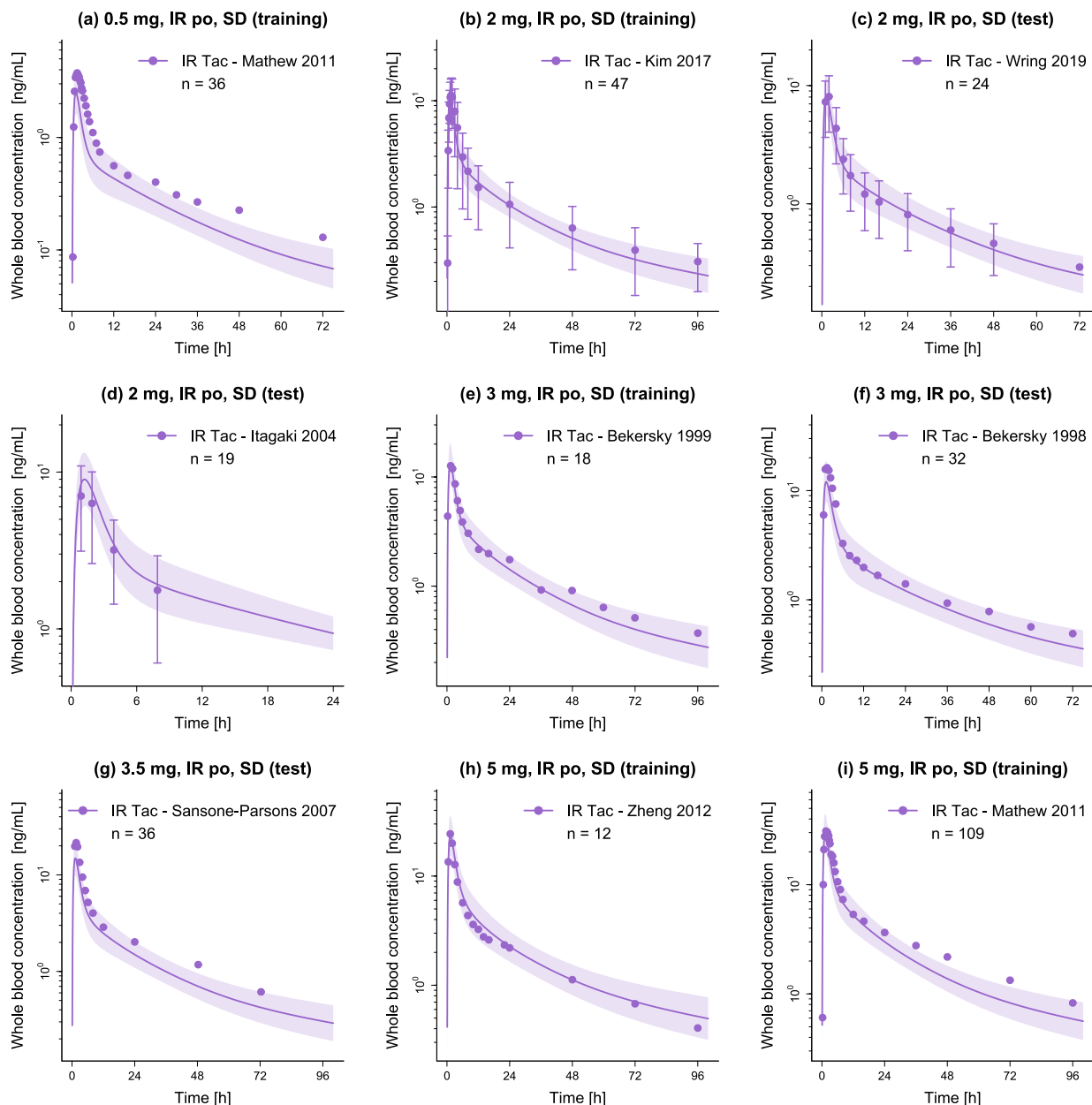


Figure S2: Semilogarithmic plots of predicted whole blood concentration-time profiles of IR tacrolimus (fasted). Solid lines and ribbons represent population predictions ($n = 1000$; geometric mean and geometric standard deviation), while corresponding observed data are shown as dots (\pm standard deviation, if available) [12–19]. IR: immediate-release, n: number of participants, po: oral, SD: single dose, Tac: tacrolimus.

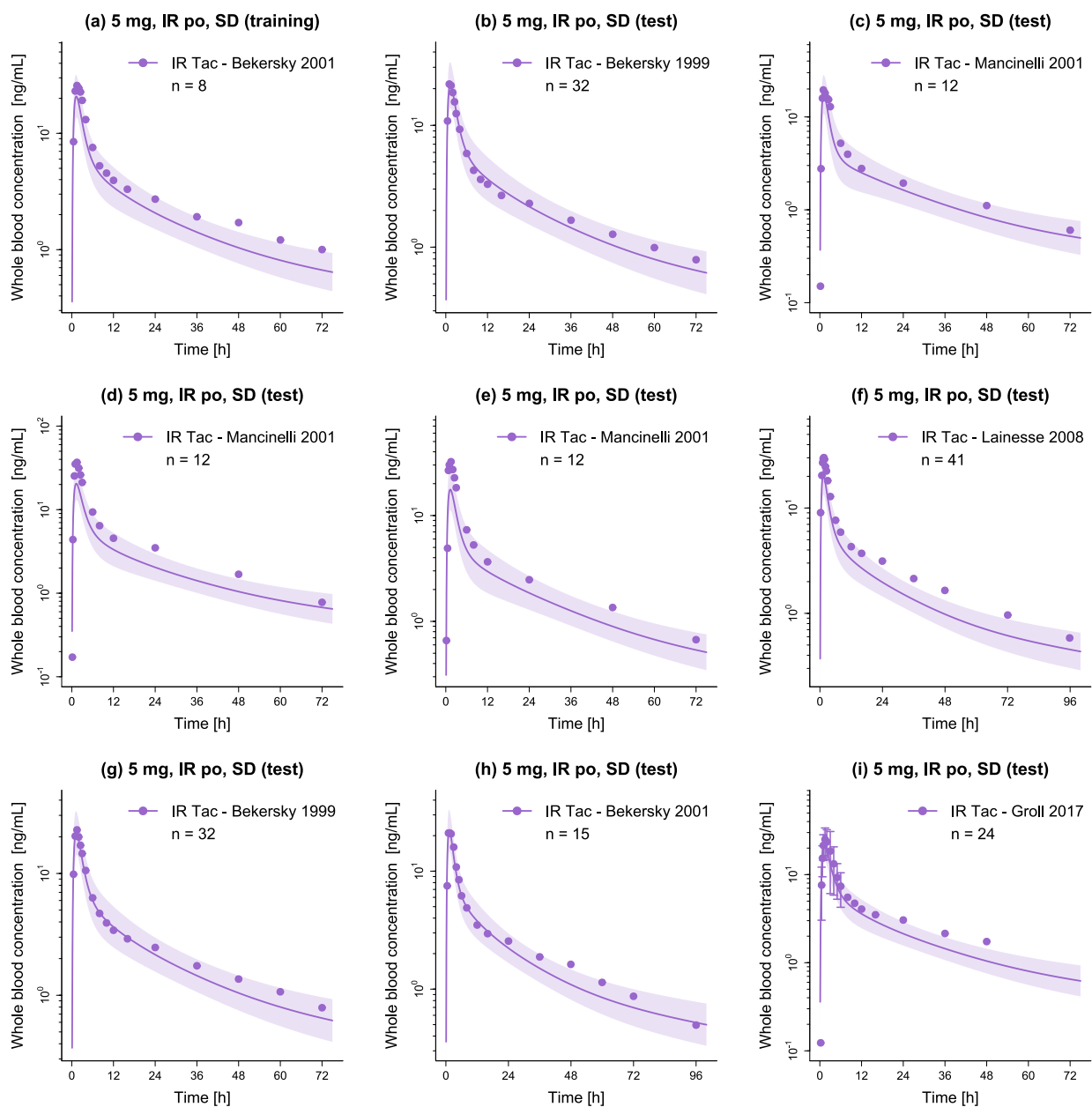


Figure S3: Semilogarithmic plots of predicted whole blood concentration-time profiles of IR tacrolimus (fasted). Solid lines and ribbons represent population predictions ($n = 1000$; geometric mean and geometric standard deviation), while corresponding observed data are shown as dots (\pm standard deviation, if available) [9, 10, 20–23]. IR: immediate-release, n: number of participants, po: oral, SD: single dose, Tac: tacrolimus.

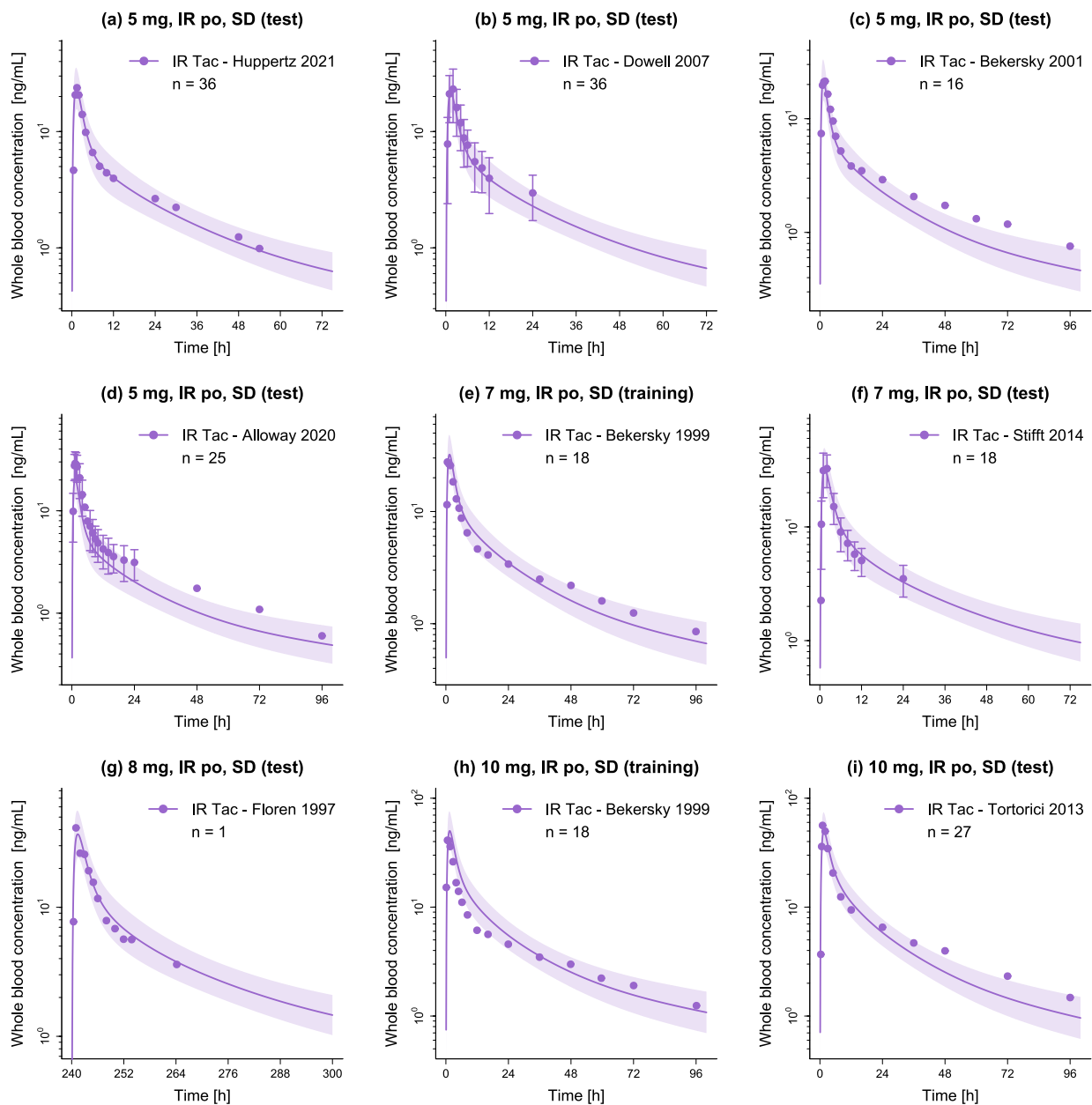


Figure S4: Semilogarithmic plots of predicted whole blood concentration-time profiles of IR tacrolimus (fasted). Solid lines and ribbons represent population predictions ($n = 1000$; geometric mean and geometric standard deviation), while corresponding observed data are shown as dots (\pm standard deviation, if available) [11, 16, 24–29]. IR: immediate-release, n: number of participants, po: oral, SD: single dose, Tac: tacrolimus.

S2.1.3 Extended-Release Oral Tacrolimus

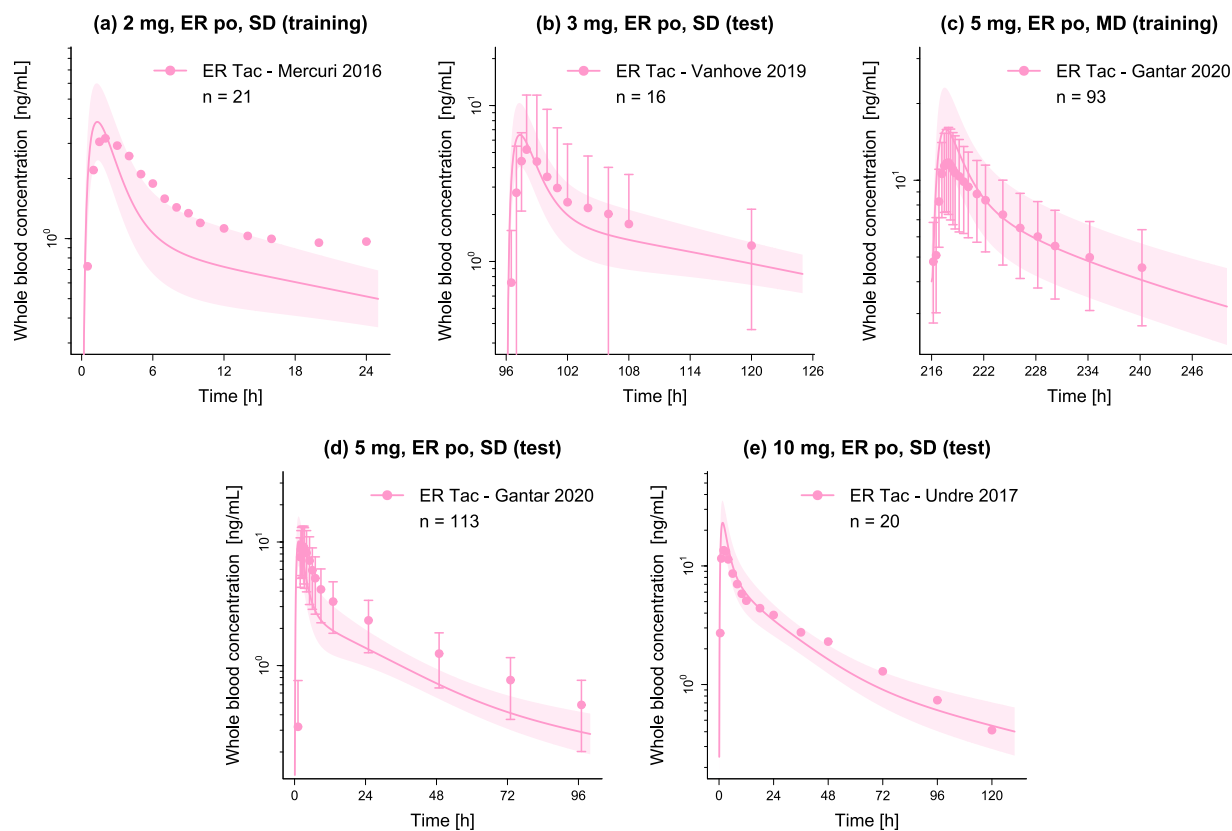


Figure S5: Semilogarithmic plots of predicted whole blood concentration-time profiles of ER tacrolimus (fasted). Solid lines and ribbons represent population predictions ($n = 1000$; geometric mean and geometric standard deviation), while corresponding observed data are shown as dots (\pm standard deviation, if available) [30–33]. ER: extended-release, MD: multiple dose, n: number of participants, po: oral, SD: single dose, Tac: tacrolimus.

S2.2 Whole Blood Concentration-Time Profiles (Linear)

S2.2.1 Intravenous Tacrolimus

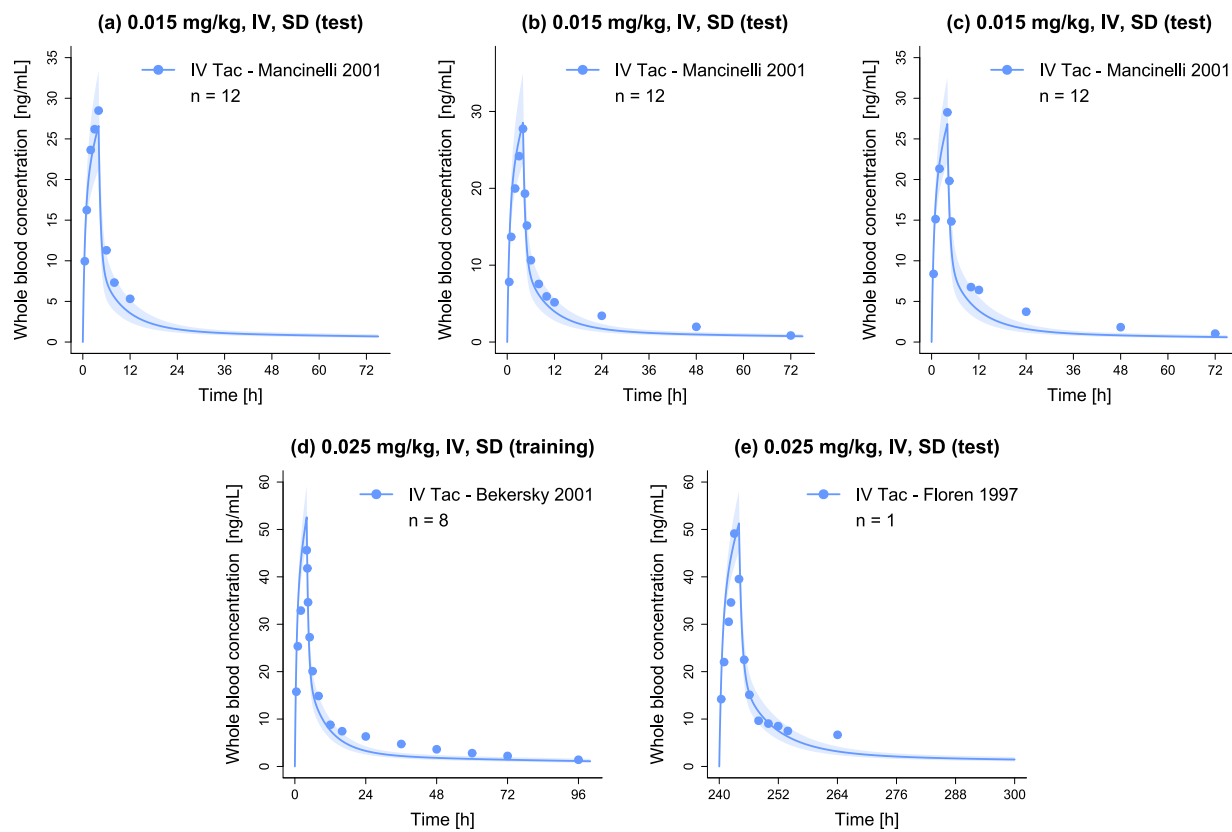


Figure S6: Linear plots of predicted whole blood concentration-time profiles of IV tacrolimus (fasted). Solid lines and ribbons represent population predictions ($n = 1000$; geometric mean and geometric standard deviation), while corresponding observed data are shown as dots [9–11]. IV: intravenous, n: number of participants, SD: single dose, Tac: tacrolimus.

S2.2.2 Immediate-Release Oral Tacrolimus

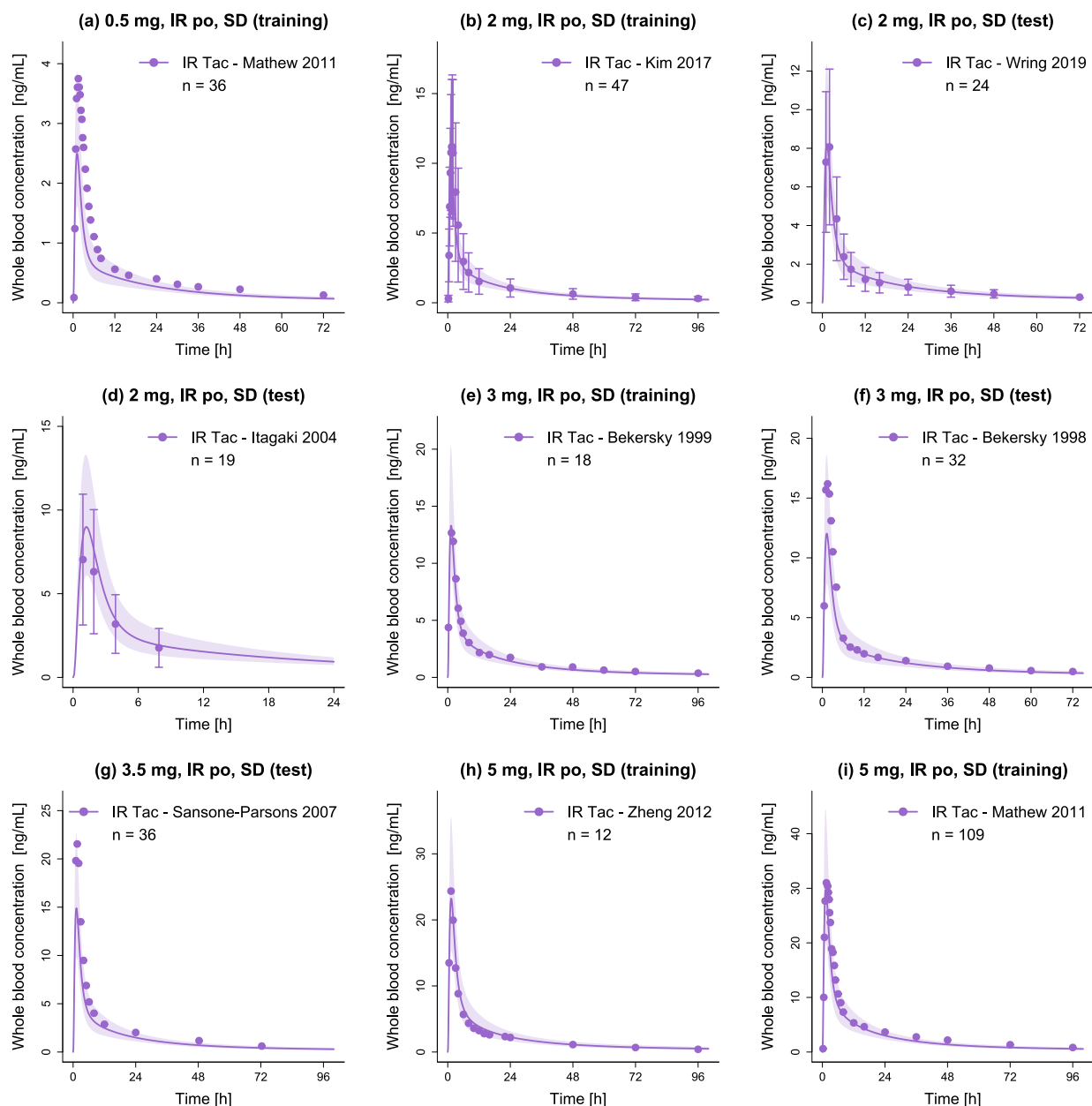


Figure S7: Linear plots of predicted whole blood concentration-time profiles of IR tacrolimus (fasted). Solid lines and ribbons represent population predictions ($n = 1000$; geometric mean and geometric standard deviation), while corresponding observed data are shown as dots (\pm standard deviation, if available) [12–19]. IR: immediate-release, n: number of participants, po: oral, SD: single dose, Tac: tacrolimus.

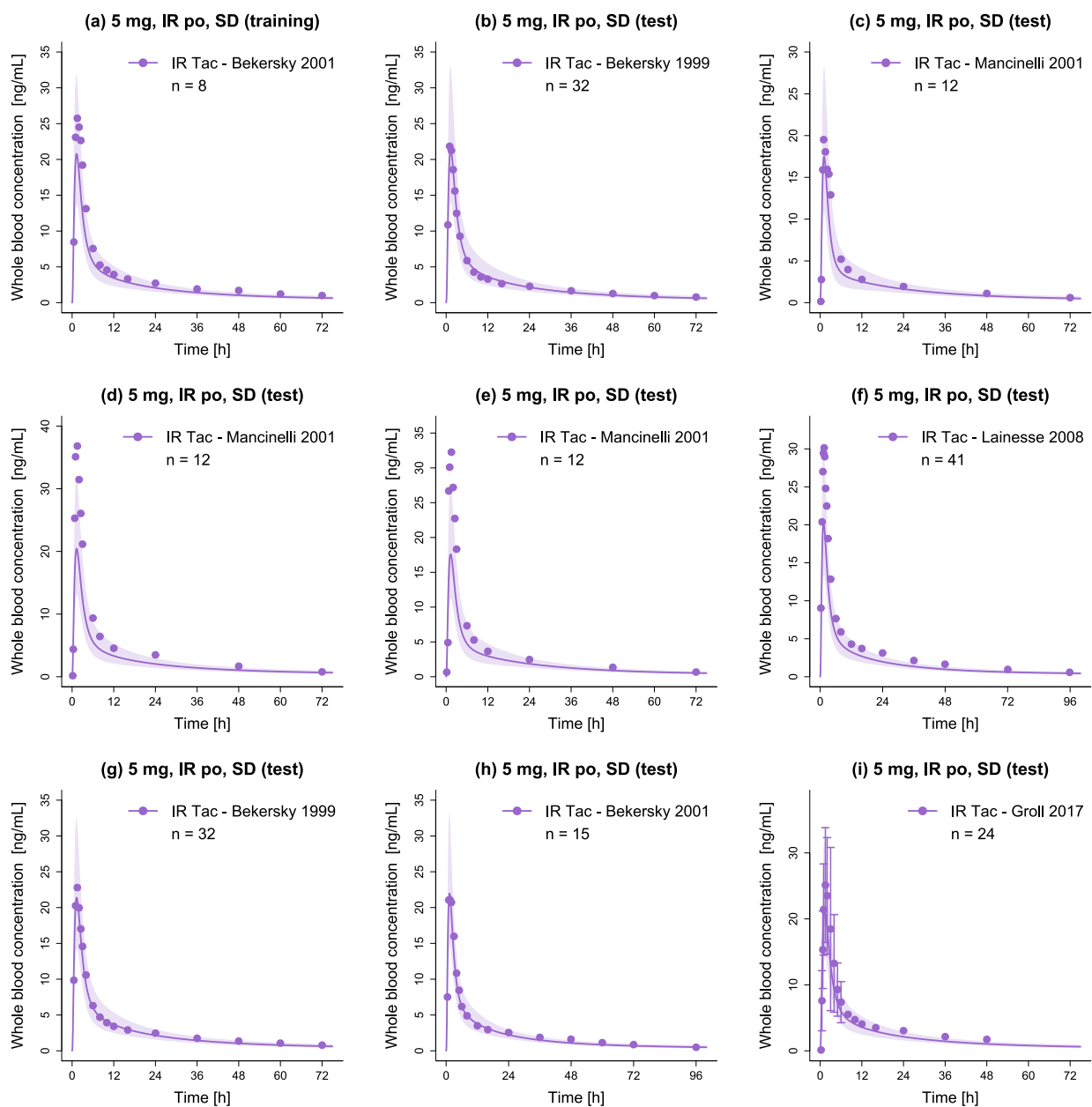


Figure S8: Linear plots of predicted whole blood concentration-time profiles of IR tacrolimus (fasted). Solid lines and ribbons represent population predictions ($n = 1000$; geometric mean and geometric standard deviation), while corresponding observed data are shown as dots (\pm standard deviation, if available) [9, 10, 20–23]. IR: immediate-release, n: number of participants, po: oral, SD: single dose, Tac: tacrolimus.

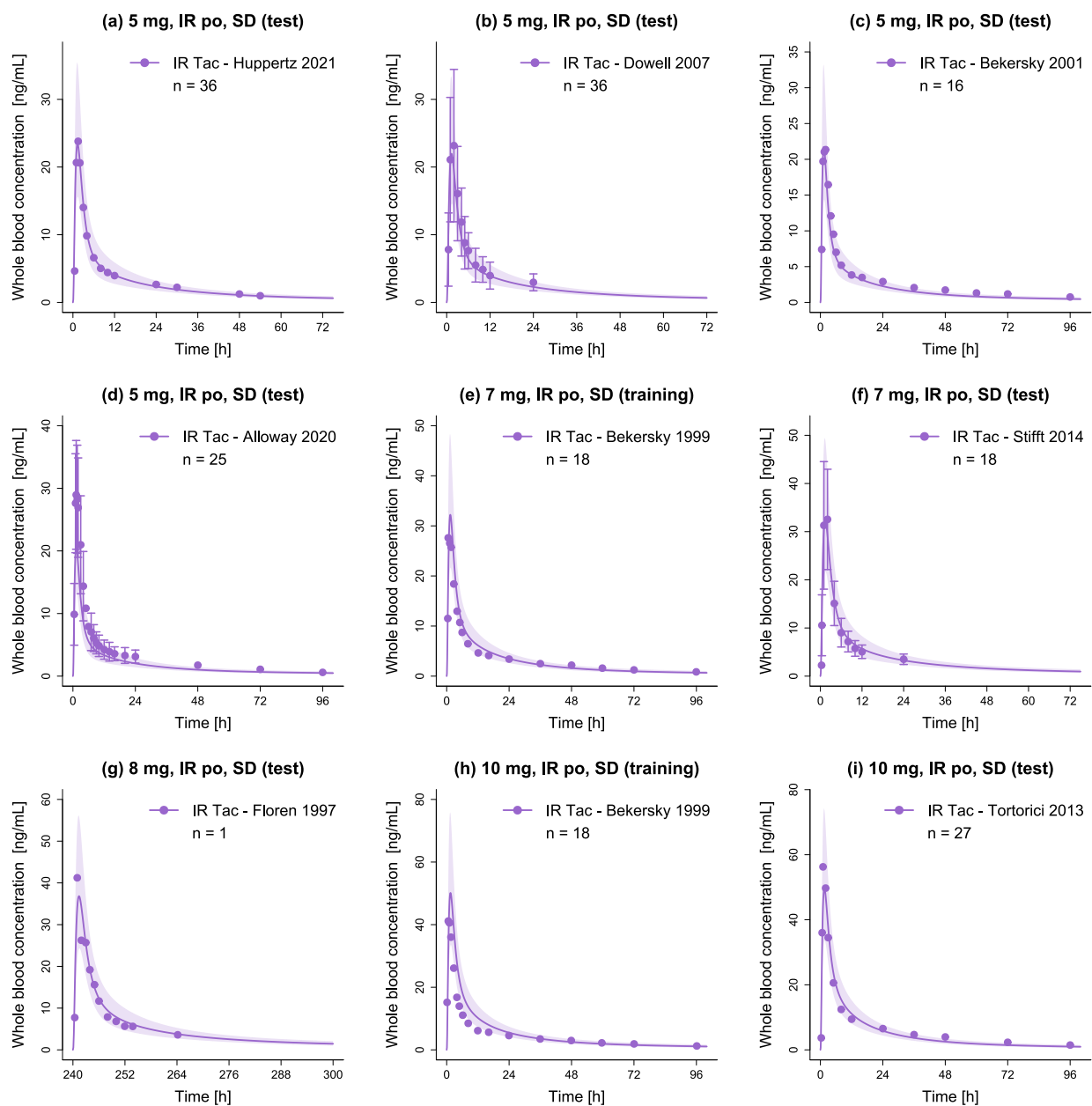


Figure S9: Linear plots of predicted whole blood concentration-time profiles of IR tacrolimus (fasted). Solid lines and ribbons represent population predictions ($n = 1000$; geometric mean and geometric standard deviation), while corresponding observed data are shown as dots (\pm standard deviation, if available) [11, 16, 24–29]. IR: immediate-release, n: number of participants, po: oral, SD: single dose, Tac: tacrolimus.

S2.2.3 Extended-Release Oral Tacrolimus

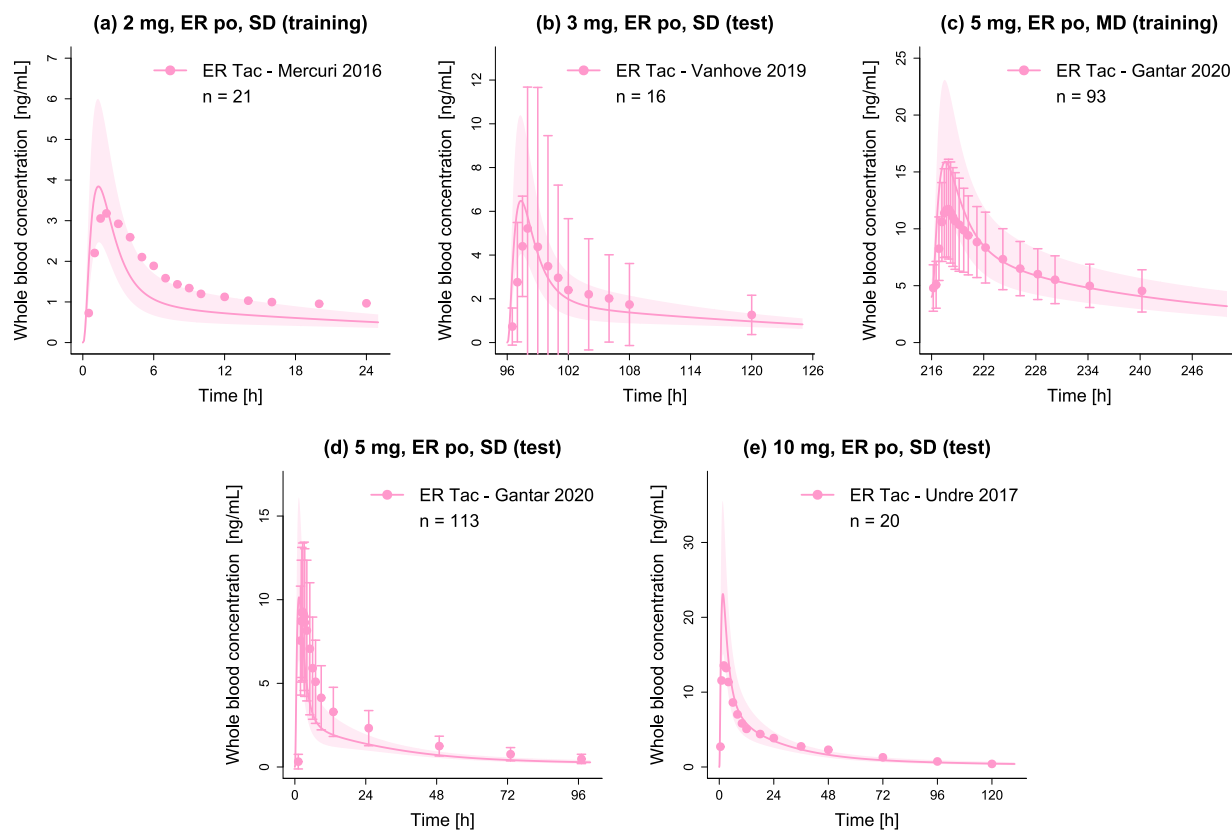


Figure S10: Linear plots of predicted whole blood concentration-time profiles of ER tacrolimus (fasted). Solid lines and ribbons represent population predictions ($n = 1000$; geometric mean and geometric standard deviation), while corresponding observed data are shown as dots (\pm standard deviation, if available) [30–33]. ER: extended-release, MD: multiple dose, n: number of participants, po: oral, SD: single dose, Tac: tacrolimus.

S2.3 Urinary Excretion Profiles

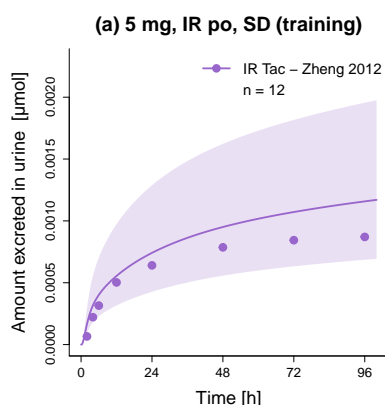


Figure S11: Cumulative amount excreted in urine of IR tacrolimus. Solid lines and ribbons represent population predictions ($n = 1000$; geometric mean and geometric standard deviation), while corresponding observed data are shown as dots [19]. IR: immediate-release, n: number of participants, po: oral, SD: single dose, Tac: tacrolimus.

S2.4 Whole Blood Concentration Goodness-of-Fit Plots

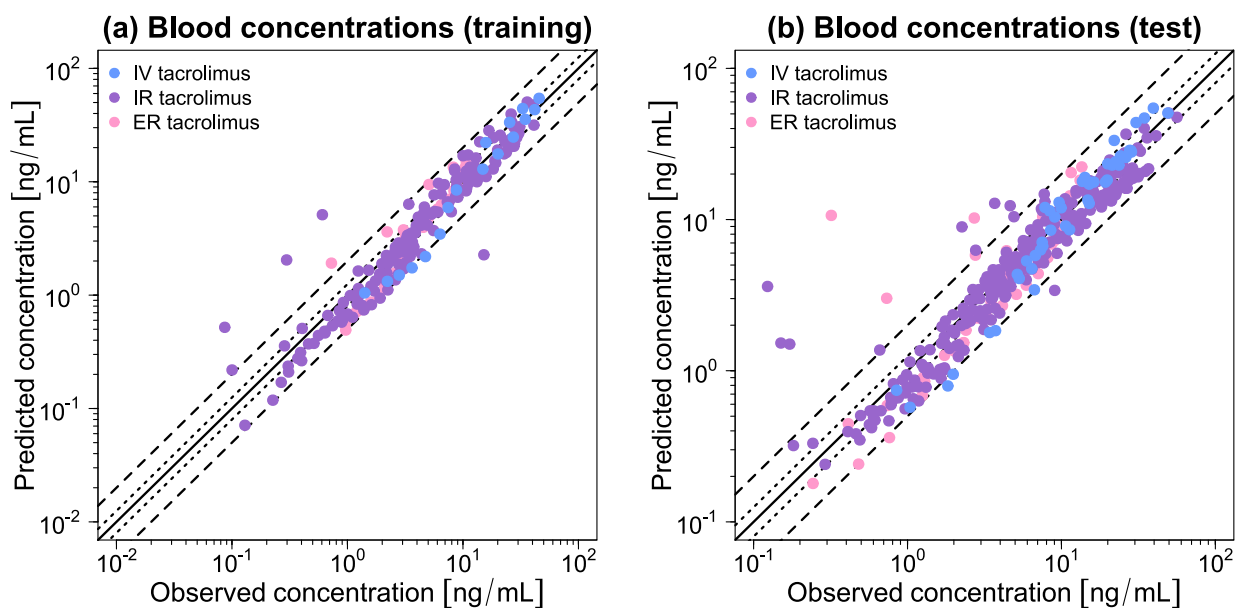


Figure S12: Goodness-of-fit plots of the final tacrolimus model. Stratified by training (a) and test dataset (b), predicted whole blood concentration measurements are plotted against corresponding observed data. The solid line represents the line of identity, while dotted lines indicate 1.25-fold and dashed lines 2-fold deviation from the respective observed value. ER: extended-release, IR: immediate-release, IV: intravenous.

S2.5 AUC_{last} and C_{max} Goodness-of-Fit Plots

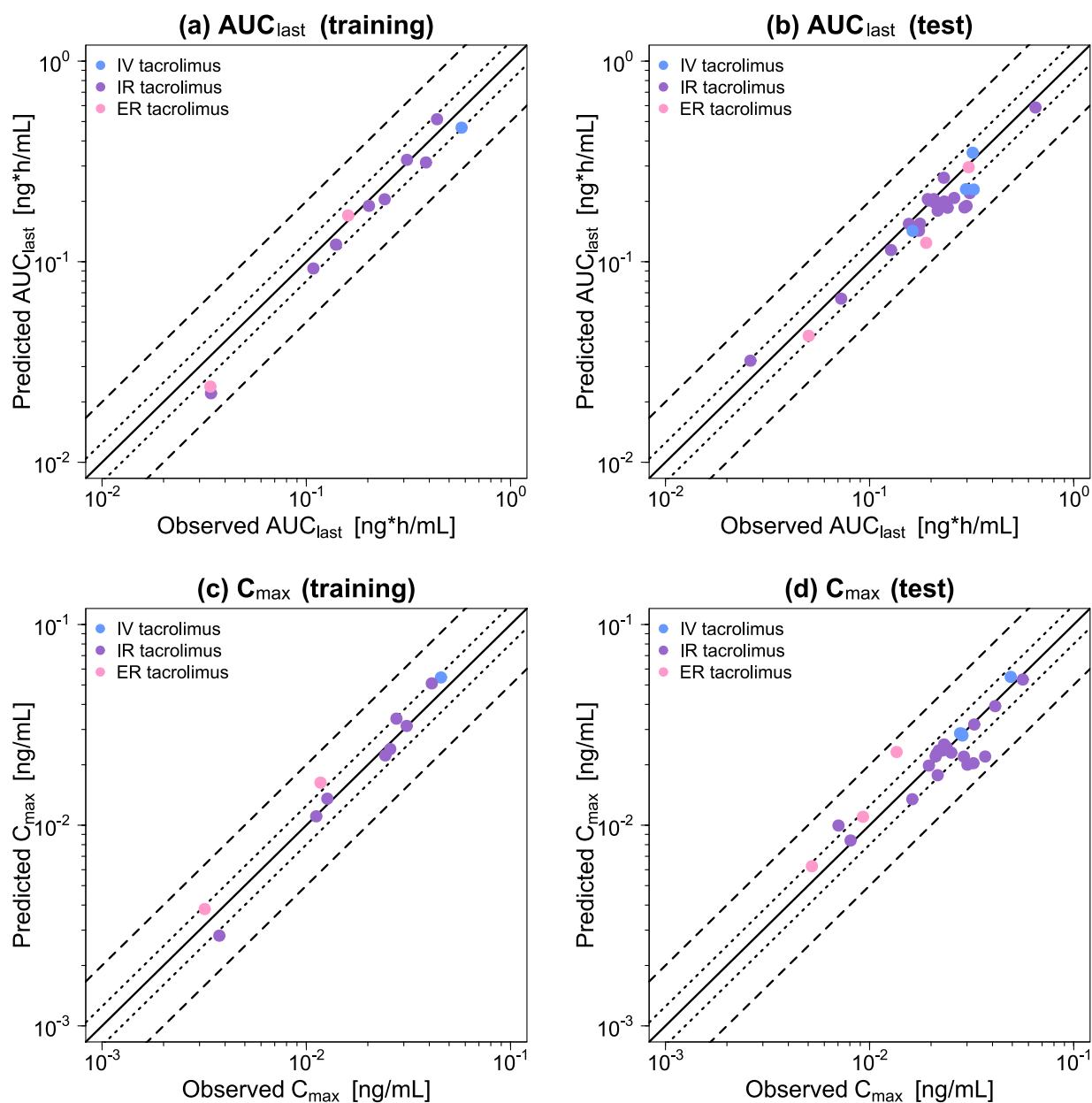


Figure S13: Goodness-of-fit plots of the final tacrolimus model. Stratified by training (left column) and test (right column) dataset, predicted AUC_{last} (a–b) and C_{max} (c–d) values are plotted against corresponding observed data. The solid line represents the line of identity, while dotted lines indicate 1.25-fold and dashed lines 2-fold deviation from the respective observed value. AUC_{last} : area under the whole blood concentration-time curve determined between first and last concentration measurements, C_{max} : maximum whole blood concentration, ER: extended-release, IR: immediate-release, IV: intravenous.

S2.6 MRD of Whole Blood Concentration Predictions

Table S5: MRD values of whole blood concentration predictions

Tacrolimus dosing regimen		n	Dataset	MRD	Reference
Route	Dose [mg]				
iv (inf, 4 h, SD)	0.015/kg	12	test	1.18	Mancinelli 2001 [9]
iv (inf, 4 h, SD)	0.015/kg	12	test	1.37	Mancinelli 2001 [9]
iv (inf, 4 h, SD)	0.015/kg	12	test	1.50	Mancinelli 2001 [9]
iv (inf, 4 h, SD)	0.025/kg	8	training	1.49	Bekersky 2001 [10]
iv (inf, 4 h, SD)	0.025/kg	1	test	1.35	Floren 1997 [11]
po (IR cap, SD)	0.5	36	training	1.81	Mathew 2011 [12]
po (IR cap, SD)	2	47	training	1.71	Kim 2017 [13]
po (IR cap, SD)	2	24	test	1.17	Wring 2019 [14]
po (IR cap, SD)	2	19	test	1.28	Itagaki 2004 [15]
po (IR cap, SD)	3	18	training	1.29	Bekersky 1999 [16]
po (IR cap, SD)	3	32	test	1.25	Bekersky 1998 [17]
po (IR cap, SD)	3.5	36	test	1.24	Sansone-Parsons 2007 [18]
po (IR cap, SD)	5	12	training	1.09	Zheng 2012 [19]
po (IR cap, SD)	5	109	training	1.68	Mathew 2011 [12]
po (IR cap, SD)	5	8	training	1.27	Bekersky 2001 [10]
po (IR cap, SD)	5	32	test	1.19	Bekersky 1999 [20]
po (IR cap, SD)	5	12	test	1.31	Mancinelli 2001 [9]
po (IR cap, SD)	5	12	test	1.53	Mancinelli 2001 [9]
po (IR cap, SD)	5	12	test	1.52	Mancinelli 2001 [9]
po (IR cap, SD)	5	41	test	1.59	Lainesse 2008 [21]
po (IR cap, SD)	5	32	test	1.17	Bekersky 1999 [20]
po (IR cap, SD)	5	15	test	1.25	Bekersky 2001 [22]
po (IR cap, SD)	5	24	test	1.27	Groll 2017 [23]
po (IR cap, SD)	5	36	test	1.32	Huppertz 2021 [24]
po (IR cap, SD)	5	36	test	1.20	Dowell 2007 [25]
po (IR cap, SD)	5	16	test	1.38	Bekersky 2001 [26]
po (IR cap, SD)	5	25	test	1.39	Alloway 2020 [27]
po (IR cap, SD)	7	18	training	1.25	Bekersky 1999 [16]
po (IR cap, SD)	7	18	test	1.57	Stift 2014 [28]
po (IR cap, SD)	8	1	test	1.28	Floren 1997 [11]
po (IR cap, SD)	10	18	training	1.75	Bekersky 1999 [16]
po (IR cap, SD)	10	27	test	1.52	Tortorici 2013 [29]
po (ER cap, SD)	2	21	training	1.73	Mercuri 2016 [30]
po (ER cap, SD)	3	16	test	1.70	Vanhove 2019 [31]
po (ER cap, MD, 10d)	5	93	training	1.31 (D10)	Gantar 2020 [32]
po (ER cap, SD)	5	113	test	2.46	Gantar 2020 [32]
po (ER cap, SD)	10	20	test	1.54	Undre 2017 [33]
Training dataset mean MRD (range)			1.49 (1.09–1.81)		
Test dataset mean MRD (range)			1.40 (1.17–2.46)		
Overall mean MRD (range)			1.43 (1.09–2.46)		
MRD \leq 2			36/37		

Cap: capsule, d: dosage period in days, D: day of pharmacokinetic sampling, ER: extended-release, inf: infusion, IR: immediate-release, iv: intravenous, MD: multiple dose (once daily), MRD: mean relative deviation, n: number of participants, po: oral, SD: single dose.

S2.7 Predicted and Observed AUC_{last} and C_{max} Values

Table S6: Predicted versus observed AUC_{last} and C_{max} values

Tacrolimus dosing regimen		n	Dataset	AUC _{last}			C _{max}			Reference
Route	Dose [mg]			Pred [$\frac{ng \cdot h}{mL}$]	Obs [$\frac{ng \cdot h}{mL}$]	Pred/Obs	Pred [$\frac{ng}{mL}$]	Obs [$\frac{ng}{mL}$]	Pred/Obs	
iv (inf, 4 h, SD)	0.015/kg	12	test	142.45	162.45	0.88	27.98	28.48	0.98	Mancinelli 2001 [9]
iv (inf, 4 h, SD)	0.015/kg	12	test	229.85	296.55	0.78	28.69	27.74	1.03	Mancinelli 2001 [9]
iv (inf, 4 h, SD)	0.015/kg	12	test	229.01	323.52	0.71	28.60	28.26	1.01	Mancinelli 2001 [9]
iv (inf, 4 h, SD)	0.025/kg	8	training	465.95	575.58	0.81	54.48	45.62	1.19	Bekersky 2001 [10]
iv (inf, 4 h, SD)	0.025/kg	1	test	349.43	319.86	1.09	54.84	49.13	1.12	Floren 1997 [11]
po (IR cap, SD)	0.5	36	training	22.08	34.14	0.65	2.82	3.75	0.75	Mathew 2011 [12]
po (IR cap, SD)	2	47	training	92.55	108.25	0.85	11.07	11.18	0.99	Kim 2017 [13]
po (IR cap, SD)	2	24	test	65.42	72.57	0.90	8.39	8.07	1.04	Wring 2019 [14]
po (IR cap, SD)	2	19	test	32.10	26.08	1.23	9.96	7.04	1.42	Itagaki 2004 [15]
po (IR cap, SD)	3	18	training	121.73	139.67	0.87	13.56	12.67	1.07	Bekersky 1999 [16]
po (IR cap, SD)	3	32	test	114.33	127.30	0.90	13.47	16.19	0.83	Bekersky 1998 [17]
po (IR cap, SD)	3.5	36	test	142.77	174.46	0.82	17.75	21.55	0.82	Sansone-Parsons 2007 [18]
po (IR cap, SD)	5	12	training	189.89	202.54	0.94	22.27	24.35	0.91	Zheng 2012 [19]
po (IR cap, SD)	5	109	training	312.54	385.23	0.81	31.24	31.01	1.01	Mathew 2011 [12]
po (IR cap, SD)	5	8	training	204.75	241.76	0.85	23.95	25.57	0.93	Bekersky 2001 [10]
po (IR cap, SD)	5	32	test	205.19	192.78	1.06	23.57	21.83	1.08	Bekersky 1999 [20]
po (IR cap, SD)	5	12	test	155.34	176.64	0.88	19.82	19.52	1.02	Mancinelli 2001 [9]
po (IR cap, SD)	5	12	test	190.20	298.74	0.64	21.99	36.81	0.60	Mancinelli 2001 [9]
po (IR cap, SD)	5	12	test	185.79	241.11	0.77	20.37	32.25	0.63	Mancinelli 2001 [9]
po (IR cap, SD)	5	41	test	186.43	291.67	0.64	20.03	30.13	0.66	Lainesse 2008 [21]
po (IR cap, SD)	5	32	test	205.20	192.78	0.99	23.57	22.79	1.03	Bekersky 1999 [20]
po (IR cap, SD)	5	15	test	199.51	232.19	0.86	22.02	21.05	1.05	Bekersky 2001 [22]
po (IR cap, SD)	5	24	test	181.67	216.42	0.84	22.98	25.12	0.91	Groll 2017 [23]
po (IR cap, SD)	5	36	test	201.69	195.87	1.03	24.46	23.80	1.03	Huppertz 2021 [24]
po (IR cap, SD)	5	36	test	154.44	155.78	0.99	25.26	23.17	1.09	Dowell 2007 [25]
po (IR cap, SD)	5	16	test	207.86	259.59	0.80	22.75	21.35	1.07	Bekersky 2001 [26]
po (IR cap, SD)	5	25	test	219.83	309.41	0.71	21.96	28.95	0.76	Alloway 2020 [27]

AUC_{last}: area under the whole blood concentration-time curve determined between first and last concentration measurements, cap: capsule, C_{max}: maximum whole blood concentration, d: dosage period in days, D: day of pharmacokinetic sampling, ER: extended-release, GMFE: geometric mean fold error, inf: infusion, IR: immediate-release, iv: intravenous, MD: multiple dose (once daily), n: number of participants, obs: observed, po: oral, pred: predicted, SD: single dose.

Table S6: Predicted versus observed AUC_{last} and C_{max} values (*continued*)

Tacrolimus dosing regimen		n	Dataset	AUC_{last}			C_{max}			Reference
Route	Dose [mg]			Pred [$\frac{ng*h}{mL}$]	Obs [$\frac{ng*h}{mL}$]	Pred/Obs	Pred [$\frac{ng}{mL}$]	Obs [$\frac{ng}{mL}$]	Pred/Obs	
po (IR cap, SD)	7	18	training	322.03	310.92	1.04	33.96	27.61	1.23	Bekersky 1999 [16]
po (IR cap, SD)	7	18	test	197.83	207.83	0.95	31.76	32.55	0.98	Stiftt 2014 [28]
po (IR cap, SD)	8	1	test	262.43	231.05	1.13	39.20	41.23	0.95	Floren 1997 [11]
po (IR cap, SD)	10	18	training	513.34	436.37	1.18	50.90	41.14	1.24	Bekersky 1999 [16]
po (IR cap, SD)	10	27	test	587.32	649.46	0.90	53.20	56.27	0.95	Tortorici 2013 [29]
po (ER cap, SD)	2	21	training	23.84	33.91	0.70	3.82	3.18	1.20	Mercuri 2016 [30]
po (ER cap, SD)	3	16	test	42.75	50.31	0.85	6.26	5.22	1.20	Vanhove 2019 [31]
po (ER cap, MD, 10d)	5	93	training	170.06	160.21	1.06 (D10)	16.29	11.73	1.39 (D10)	Gantar 2020 [32]
po (ER cap, SD)	5	113	test	124.18	189.24	0.66	11.02	9.28	1.19	Gantar 2020 [32]
po (ER cap, SD)	10	20	test	295.89	305.64	0.97	23.16	12.56	1.71	Undre 2017 [33]
Training dataset mean GMFE (range)				1.21 (1.04–1.55)			1.17 (1.01–1.39)			
Test dataset mean GMFE (range)				1.21 (1.01–1.57)			1.19 (1.01–1.71)			
Overall mean GMFE (range)				1.21 (1.01–1.57)			1.18 (1.01–1.71)			
GMFE ≤ 2				37/37			37/37			

AUC_{last} : area under the whole blood concentration-time curve determined between first and last concentration measurements, cap: capsule, C_{max} : maximum whole blood concentration, d: dosage period in days, D: day of pharmacokinetic sampling, ER: extended-release, GMFE: geometric mean fold error, inf: infusion, IR: immediate-release, iv: intravenous, MD: multiple dose (once daily), n: number of participants, obs: observed, po: oral, pred: predicted, SD: single dose.

S2.8 Local Sensitivity Analysis

S2.8.1 Methods

A local sensitivity analysis was performed for each modeled formulation, by calculating the sensitivity to single parameter changes according to Equation S2. A relative perturbation of 1000% was applied (variation range 10.0, maximum number of 9 steps) and parameters included were either optimized or assumed to affect AUC_{last} .

$$S = \frac{\Delta AUC_{last}}{\Delta p} \cdot \frac{p}{AUC_{last}} \quad (S2)$$

where S = sensitivity, ΔAUC_{last} = change of AUC_{last} , Δp = change of the analyzed parameter value, p = original parameter value, and AUC_{last} = simulated AUC_{last} with the original parameter value.

The threshold for sensitivity was set at $|0.5|$, which corresponds to a 50% change in simulated AUC_{last} given a 100% change in the parameter value examined.

S2.8.2 Results

Table S7: Parameters evaluated during the local sensitivity analyses

Parameter	Source	Parameter	Source
CYP3A4 K_i CI	Literature	Lipophilicity	Optimized
CYP3A4 K_I MBI	Literature	Solubility	Literature
CYP3A4 K_i MBI	Literature	GFR fraction	Assumed
CYP3A4 k_{inact} MBI	Literature	Dissolution shape IR Tac	Optimized
CYP3A5 K_I MBI	Literature	Dissolution time IR Tac	Literature
CYP3A5 K_i MBI	Literature	Dissolution shape ER Tac	Optimized
CYP3A5 k_{inact} MBI	Literature	Dissolution time ER Tac	Optimized
Intestinal permeability IR Tac	Optimized	CYP3A4 K_M	Literature
Intestinal permeability ER Tac	Optimized	CYP3A5 K_M	Literature
pKa, acid	Literature	CYP3A4 k_{cat}	Optimized
f_u	Literature	CYP3A5 k_{cat}	Optimized

CI: competitive inhibition, CYP: cytochrome P450, ER: extended-release, f_u : fraction unbound, GFR: glomerular filtration rate, IR: immediate-release, k_{cat} : catalytic rate constant, K_i : dissociation constant inhibitor-enzyme complex, K_I : concentration for half-maximal inactivation, k_{inact} : maximum inactivation rate constant, K_M : Michaelis-Menten constant, MBI: mechanism-based inactivation, pKa: acid dissociation constant, Tac: tacrolimus.

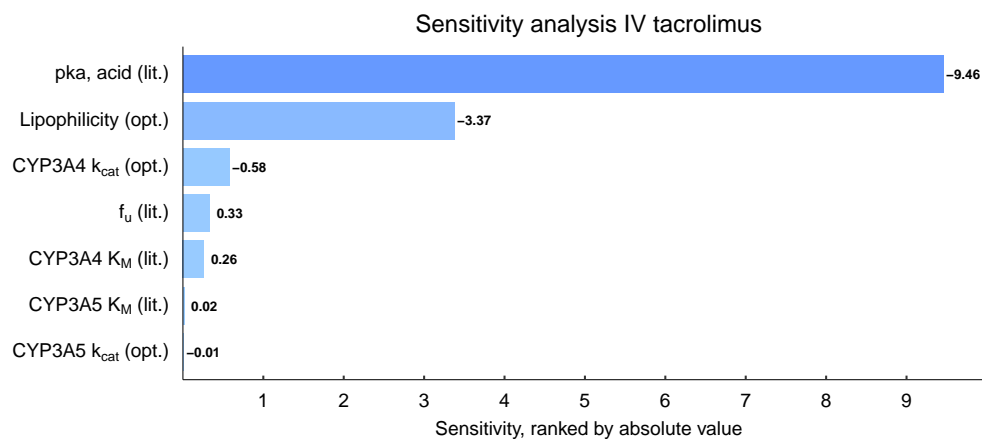


Figure S14: IV tacrolimus model sensitivity analysis (0.025 mg/kg body weight, 4 h infusion, single dose [10]). Presented are parameters with a calculated sensitivity different from 0.00. CYP: cytochrome P450, f_u : fraction unbound, IV: intravenous, k_{cat} : catalytic rate constant, K_M : Michaelis-Menten constant, lit.: literature, opt.: optimized, pKa: acid dissociation constant.

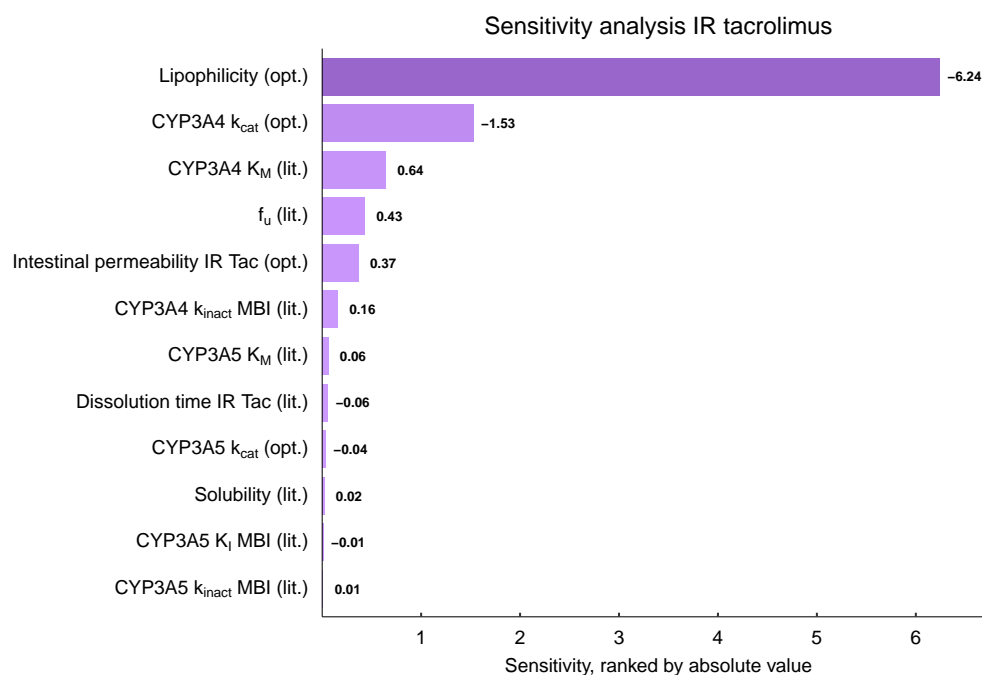


Figure S15: IR tacrolimus model sensitivity analysis (10 mg, single dose [16]). Presented are parameters with a calculated sensitivity different from 0.00. CYP: cytochrome P450, f_u : fraction unbound, IR: immediate-release, k_{cat} : catalytic rate constant, K_I : concentration for half-maximal inactivation, k_{inact} : maximum inactivation rate constant, K_M : Michaelis-Menten constant, lit.: literature, MBI: mechanism-based inactivation, opt.: optimized, Tac: tacrolimus.

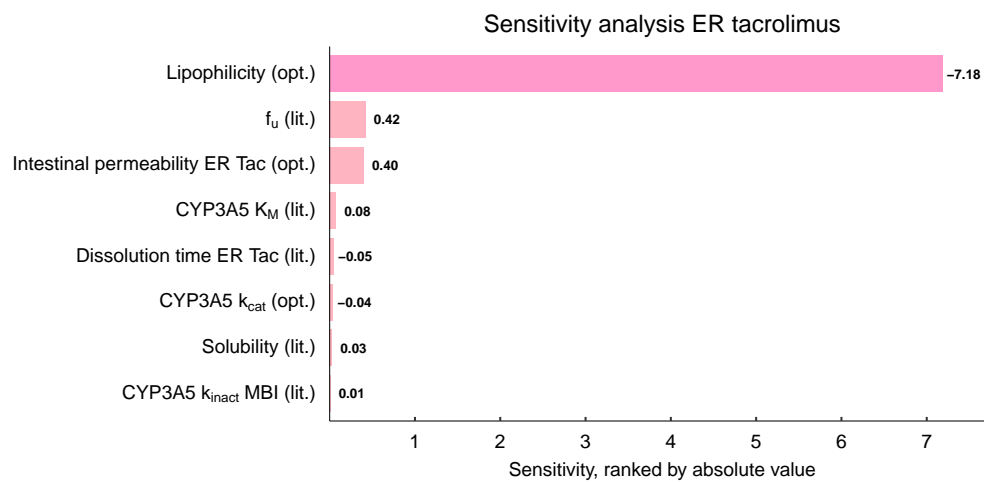


Figure S16: ER tacrolimus model sensitivity analysis (10 mg, single dose [33]). Presented are parameters with a calculated sensitivity different from 0.00. CYP: cytochrome P450, ER: extended-release, f_u : fraction unbound, k_{cat} : catalytic rate constant, k_{inact} : maximum inactivation rate constant, K_M : Michaelis-Menten constant, lit.: literature, MBI: mechanism-based inactivation, opt.: optimized, Tac: tacrolimus.

S3 Food-Drug Interaction Modeling

Modulated absorption and distribution of tacrolimus due to food intake was implemented via adjustment of the Weibull parameters time (50% dissolved) and shape, as well as the intestinal permeability. The final model parameters are listed in Table S3.

S3.1 Clinical Study Data

Table S8: Tacrolimus FDI model study table

Tacrolimus dosing regimen		n	Females [%]	Ethnicity ^a	Frequency ^a of <i>CYP3A5*1</i> [%]	Age [years]	Weight [kg]	Height [cm]	Dataset	Reference
Route	Dose [mg]									
po (IR cap, SD, fasted)	5	36	50	European	7.8	27±8.3	72±13	173±9	test	Huppertz 2021 [24]
po (IR cap, SD, fed) after 622 kcal	5	36	50	European	7.8	27±8.3	72±13	173±9	test	Huppertz 2021 [24]
po (IR cap, SD, fasted)	5	15	0	White American	7.8	32.6±10.1 (20–45)	85.2±9.42 (70.9–102)	179±5.77 (170–190)	test	Bekersky 2001 [22]
po (IR cap, SD, fed) 0.33 h after 668 kcal	5	15	0	White American	7.8	32.6±10.1 (20–45)	85.2±9.42 (70.9–102)	179±5.77 (170–190)	training	Bekersky 2001 [22]
po (IR cap, SD, fasted)	5	16	0	White American	7.8	34±9.23 (22–45)	82.5±10.3 (64.1–100)	183±6.48 (173–193)	test	Bekersky 2001 [26]
po (IR cap, SD, fed) 0.33 h after 848 kcal	5	16	0	White American	7.8	34±9.23 (22–45)	82.5±10.3 (64.1–100)	183±6.48 (173–193)	test	Bekersky 2001 [26]
po (IR cap, SD, fasted)	5	16	0	White American	7.8	34±9.23 (22–45)	82.5±10.3 (64.1–100)	183±6.48 (173–193)	test	Bekersky 2001 [26]
po (IR cap, SD, fed) 1.5 h after 848 kcal	5	16	0	White American	7.8	34±9.23 (22–45)	82.5±10.3 (64.1–100)	183±6.48 (173–193)	test	Bekersky 2001 [26]

^a: implemented, cap: capsule, CYP: cytochrome P450, FDI: food-drug interaction, IR: immediate-release, kcal: kilocalories, n: number of participants, po: oral, SD: single dose; values for age, weight and height are shown as mean ± standard deviation (range).

Table S8: Tacrolimus FDI study table (*continued*)

Tacrolimus dosing regimen		n	Females [%]	Ethnicity ^a	Frequency ^a of <i>CYP3A5*1</i> [%]	Age [years]	Weight [kg]	Height [cm]	Dataset	Reference
Route	Dose [mg]									
po (IR cap, SD, fasted)	5	15	0	White American	7.8	32.6±10.1 (20–45)	85.2±9.42 (70.9–102)	179±5.77 (170–190)	test	Bekersky 2001 [22]
po (IR cap, SD, fed) 0.33 h after 849 kcal	5	15	0	White American	7.8	32.6±10.1 (20–45)	85.2±9.42 (70.9–102)	179±5.77 (170–190)	training	Bekersky 2001 [22]
po (IR cap, SD, fasted)	5	41	81	White American	7.8	47±13 (21–66)	68.0±8.3 (53.1–85.5)	164.8±7.4 (151.5–180.5)	test	Lainesse 2008 [21]
po (IR cap, SD, fed) 0.5 h after 1000 kcal	5	46	61	White American	7.8	43±12 (19–61)	65.5±9.4 (45.6–85.6)	166.0±8.6 (149.0–181.5)	test	Lainesse 2008 [21]

^a: implemented, cap: capsule, CYP: cytochrome P450, FDI: food-drug interaction, IR: immediate-release, kcal: kilocalories, n: number of participants, po: oral, SD: single dose; values for age, weight and height are shown as mean ± standard deviation (range).

S3.2 Whole Blood Concentration-Time Profiles (Semilogarithmic)

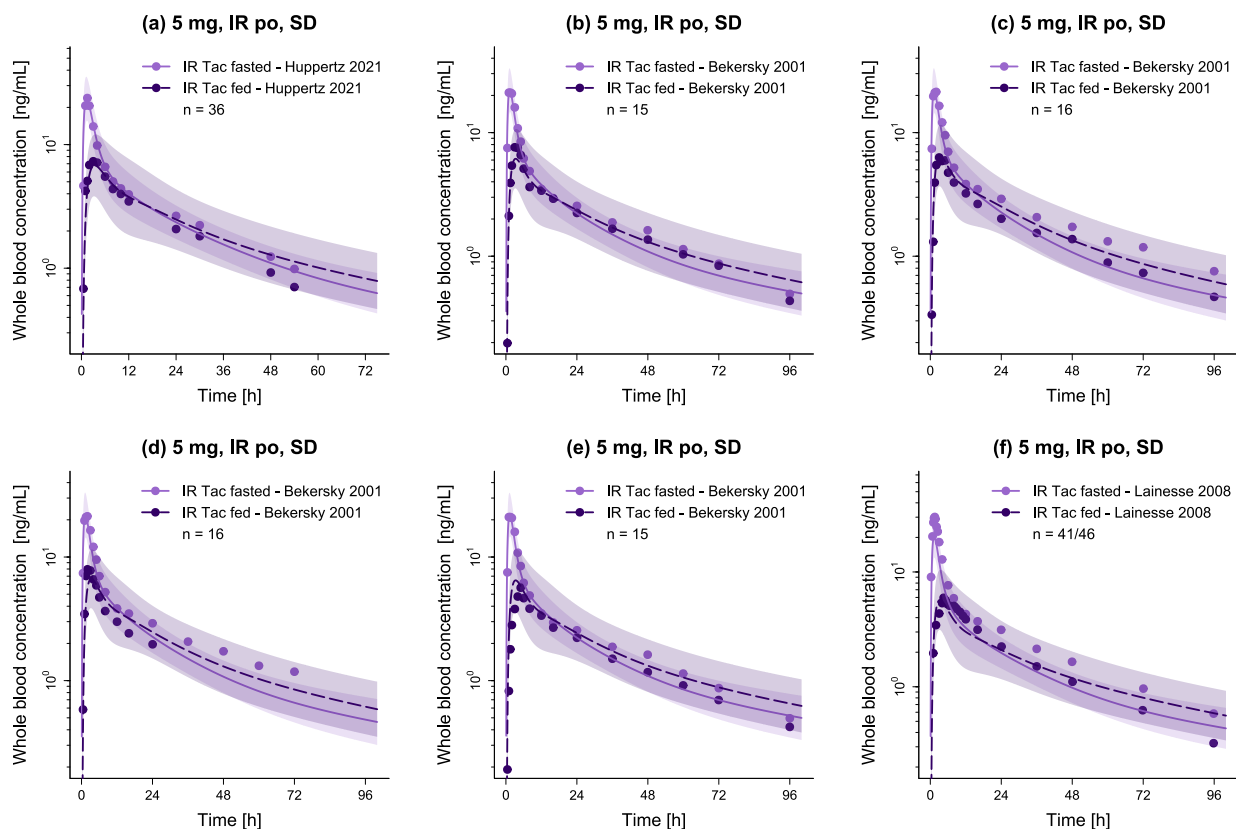


Figure S17: Evaluation of the modeled food-drug interactions. Presented are predicted whole blood concentration-time profiles (semilogarithmic plots) of IR tacrolimus under fed and fasted conditions, alongside corresponding observed data [21, 22, 24, 26]. Dashed (fed) and solid (fasted) lines and ribbons represent population predictions ($n = 1000$; geometric mean and geometric standard deviation), while corresponding observed data are shown as dots. n: number of participants, IR: immediate-release, po: oral, SD: single dose, Tac: tacrolimus.

S3.3 Whole Blood Concentration-Time Profiles (Linear)

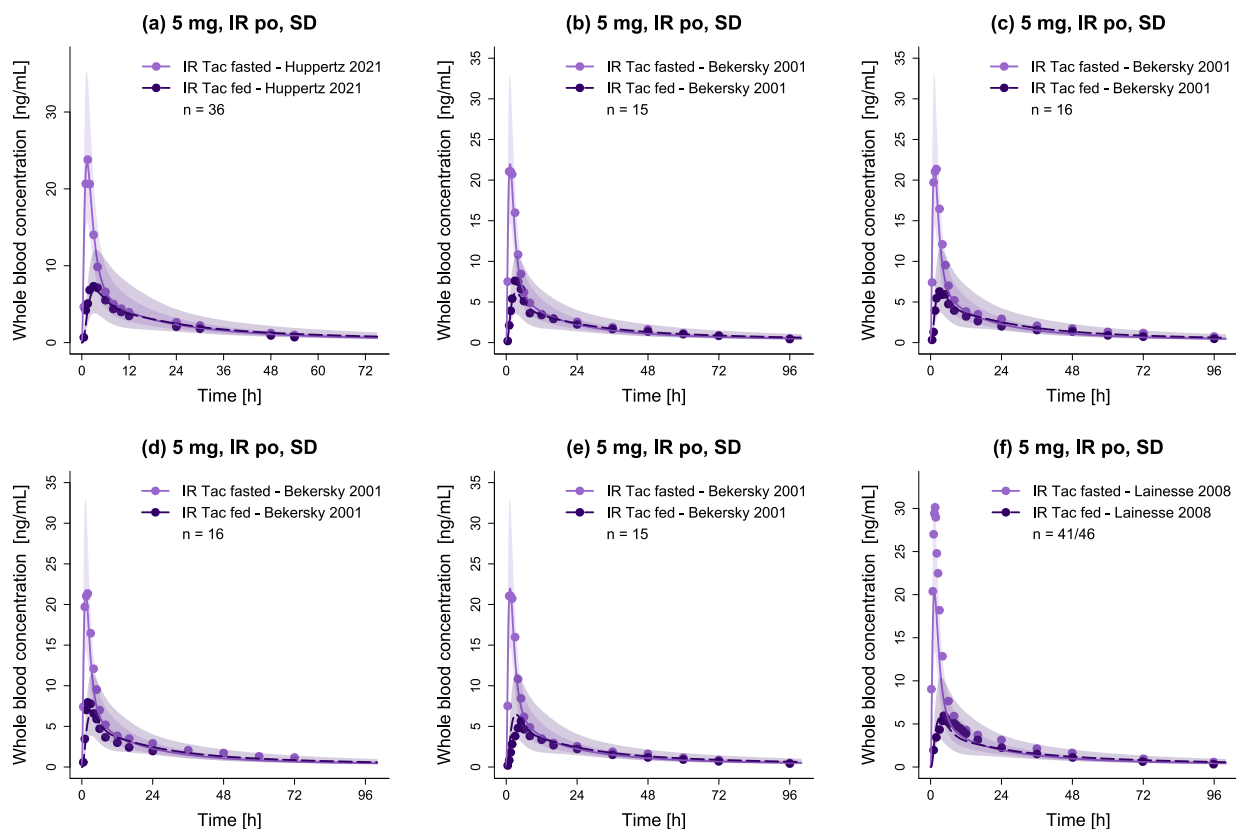


Figure S18: Evaluation of the modeled food-drug interactions. Presented are predicted whole blood concentration-time profiles (linear plots) of IR tacrolimus under fed and fasted conditions, alongside corresponding observed data [21, 22, 24, 26]. Dashed (fed) and solid (fasted) lines and ribbons represent population predictions ($n = 1000$; geometric mean and geometric standard deviation), while corresponding observed data are shown as dots. n : number of participants, IR: immediate-release, po: oral, SD: single dose, Tac: tacrolimus.

S3.4 FDI AUC_{last} and FDI C_{max} Ratio Goodness-of-Fit Plots

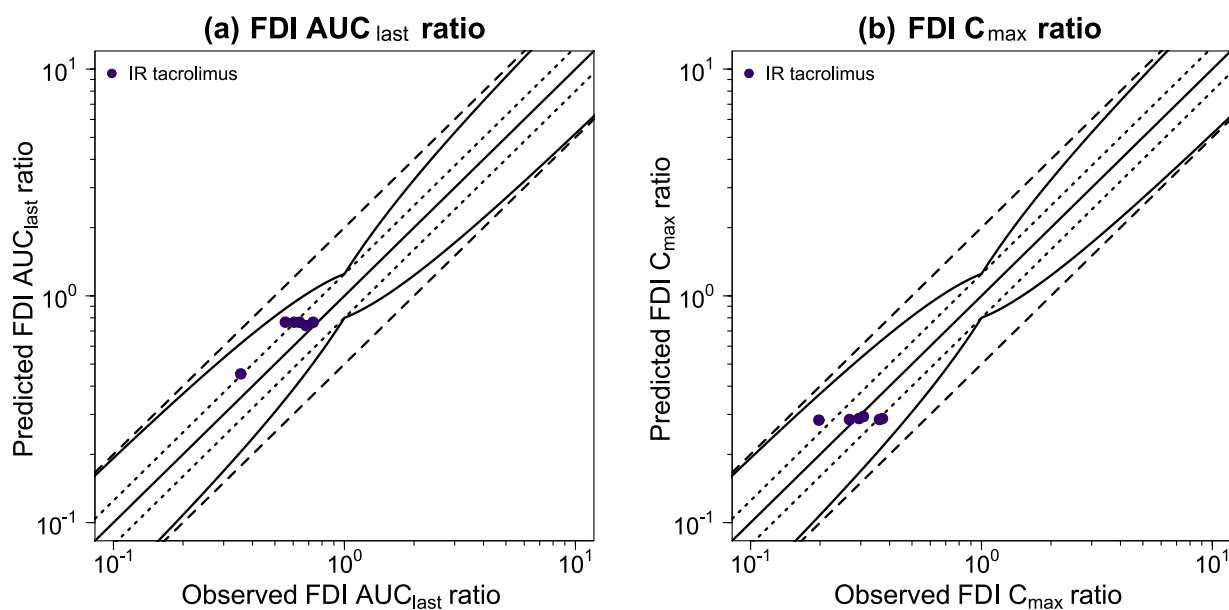


Figure S19: Evaluation of the modeled food-drug interactions. Presented are predicted versus observed FDI AUC_{last} (a) and FDI C_{max} (b) ratios with the solid line representing the line of identity, dotted lines indicating 1.25-fold and dashed lines 2-fold deviation from the respective observed value, along with the curved lines marking the prediction success limits proposed by Guest et al. [46] including 20%. AUC_{last} : area under the whole blood concentration-time curve determined between first and last concentration measurements, C_{max} : maximum whole blood concentration, FDI: food-drug interaction, n: number of participants, IR: immediate-release.

S3.5 Predicted and Observed FDI AUC_{last} and FDI C_{max} Ratios

Table S9: Predicted versus observed FDI AUC_{last} and FDI C_{max} ratios

Tacrolimus dosing regimen			n	Dataset	FDI AUC_{last} ratio			FDI C_{max} ratio			Reference
Route	Dose [mg]				Pred	Obs	Pred/Obs	Pred	Obs	Pred/Obs	
po (IR cap, SD) after 622 kcal	5	36 fasted/36 fed	test	0.74	0.68	1.08	0.29	0.31	0.95	Huppertz 2021 [24]	
po (IR cap, SD) 0.33 h after 668 kcal	5	15 fasted/15 fed	training	0.76	0.73	1.05	0.28	0.36	0.79	Bekersky 2001 [22]	
po (IR cap, SD) 0.33 h after 848 kcal	5	16 fasted/16 fed	test	0.77	0.61	1.26	0.29	0.29	0.98	Bekersky 2001 [26]	
po (IR cap, SD) 1.5 h after 848 kcal	5	16 fasted/ 16 fed	test	0.45	0.36	1.27	0.29	0.37	0.77	Bekersky 2001 [26]	
po (IR cap, SD) 0.33 h after 849 kcal	5	15 fasted/15 fed	training	0.76	0.64	1.20	0.28	0.27	1.06	Bekersky 2001 [22]	
po (IR cap, SD) 0.5 h after 1000 kcal	5	41 fasted/46 fed	test	0.77	0.55	1.38	0.28	0.20	1.43	Lainesse 2008 [21]	
Training Dataset mean GMFE (range)					1.12 (1.05–1.20)			1.17 (1.06–1.27)			
Test Dataset mean GMFE (range)					1.25 (1.08–1.38)			1.20 (1.02–1.43)			
Overall mean GMFE (range)					1.21 (1.05–1.38)			1.19 (1.02–1.43)			
GMFE ≤ 2					6/6			6/6			

AUC_{last} : area under the whole blood concentration-time curve determined between first and last concentration measurements, cap: capsule, C_{max} : maximum whole blood concentration, GMFE: geometric mean fold error, FDI: food-drug interaction, IR: immediate-release, kcal: kilocalories, n: number of participants, obs: observed, po: oral, pred: predicted, SD: single dose.

S4 Drug-Drug(-Gene) Interaction Modeling

S4.1 Types of Interactions Implemented

S4.1.1 Competitive Inhibition

Competitive inhibition (CI) involves reversible binding of an inhibitor to the respective enzyme, thus competing with substrates for the binding site, increasing the apparent Michaelis-Menten constant ($K_{M,app}$) while leaving the maximum reaction velocity (v_{max}) unaltered (Equations S3 and S4) [47]. Due to its reversibility, the inhibition can be overcome through an increase in substrate concentration (concentration-dependent inhibition).

$$v = \frac{v_{max} \cdot [S]}{K_{M,app} + [S]} \quad (S3)$$

$$K_{M,app} = K_M \cdot \left(1 + \frac{[I]}{K_i}\right) \quad (S4)$$

where v = reaction velocity, v_{max} = maximum reaction velocity, $[S]$ = free substrate concentration, $K_{M,app}$ = apparent Michaelis-Menten constant (inhibitor present), K_M = Michaelis-Menten constant (inhibitor absent), $[I]$ = free inhibitor concentration, and K_i = dissociation constant inhibitor-enzyme complex.

S4.1.2 Mechanism-Based Inactivation

In the case of mechanism-based inactivation (MBI), the inactivator, in addition to reversibly binding to the enzyme in question, is irreversibly converted into a reactive species that forms a covalent complex with the respective target (time-dependent inhibition). Due to the irreversibility, MBI can only be reversed by *de novo* synthesis of the relevant enzyme or transporter. In PK-Sim[®], MBI and its resulting impact on enzyme turnover is implemented according to Equation S5 [47].

$$\frac{d[T]}{dt} = k_{deg} \cdot [T]_0 - \left(k_{deg} + \frac{k_{inact} \cdot [I]}{K_I + [I]}\right) \cdot [T] \quad (S5)$$

where $d[T]/dt$ = enzyme turnover, k_{deg} = degradation rate constant, $[T]_0$ = initial enzyme concentration at time 0, k_{inact} = maximum inactivation rate constant, K_I = concentration for half-maximal inactivation, $[I]$ = free inactivator concentration, and $[T]$ = enzyme concentration.

S4.1.3 Induction

Induction of enzymes is usually caused by activation of specific nuclear receptors through binding of an inducer, resulting in increased *de novo* synthesis of the enzyme of interest. Equation S6 describes the correlation between maximum induction effect (E_{max}), concentration for half-maximal induction (EC_{50}) and the magnitude of induction, with the first two parameters used for implementation of an induction process in PK-Sim[®] [47, 48].

$$E = \frac{E_{max} \cdot [Ind]}{EC_{50} + [Ind]} \quad (S6)$$

where E = magnitude of induction, E_{max} = maximum induction effect, $[Ind]$ = free inducer concentration (steady-state), and EC_{50} = concentration for half-maximal induction.

S4.2 Clinical Study Data

Table S10: Tacrolimus DD(G)I model study table

Tacrolimus application [mg]	Perpetrator	Perpetrator application [mg]	n	Females [%]	Ethnicity ^a	Frequency ^a of <i>CYP3A5*1</i> [%]	Age [years]	Weight [kg]	Height [cm]	Reference
d4: 3 po (IR cap, SD)	Voriconazole	d1: 400 d2–4: 200 po (tab, BID)	6 NM CYP2C19	0	Japanese	25.8	27.7 (23–38)	63.9 (57.4–68.7)	172.7 (167.6–178.9)	Imamura 2016 [49]
d4: 3 po (IR cap, SD)	Voriconazole	d1: 400 d2–4: 200 po (tab, BID)	6 IM CYP2C19	0	Japanese	25.8	28.7 (22–37)	65.2 (57.0–74.3)	173.6 (170.0–178.5)	Imamura 2016 [49]
d4: 3 po (IR cap, SD)	Voriconazole	d1: 400 d2–4: 200 po (tab, BID)	6 PM CYP2C19	0	Japanese	25.8	27.7 (22–36)	61.3 (57.0–74.3)	174.3 (166.7–182.3)	Imamura 2016 [49]
d2: 3 po (IR cap, SD)	Voriconazole ^b	d1: 400 d2–4: 200 po (tab, BID)	18	0	European	16.7	34±11	82±13	182±8	Huppertz 2019 [50]
d5: 3 po (ER cap, SD)	Itraconazole ^c	d1–4: 200 po (cap, BID)	16	0	European	15.6	(18–28)	-	-	Vanhove 2019 [31]
d8: 0.025/kg iv (inf, 4 h, SD)	Rifampicin	d1–18: 600 po (cap, MD)	1	0	White American	100	-	-	-	Hebert 1999 [51]
d8: 8 po (IR cap, SD)	Rifampicin	d1–18: 600 po (cap, MD)	1	0	White American	100	-	-	-	Hebert 1999 [51]

–: not given, ^a: implemented, ^b: plus midazolam (not included in the model): d2; 0.03 mg; po (solution, SD), ^c: plus midazolam (not included in the model): d5; 2 mg; po (solution, SD), BID: multiple dose (twice daily), cap: capsule, CYP: cytochrome P450, d: day, DD(G)I: drug-drug(-gene) interaction, ER: extended-release, IM: intermediate metabolizer, inf: infusion, IR: immediate-release, iv: intravenous, MD: multiple dose (once daily), n: number of participants, NM: normal metabolizer, PM: poor metabolizer, po: oral, SD: single dose, tab: tablet; values for age, weight and height are presented as mean ± standard deviation (range).

S4.3 Drug-dependent Parameters DD(G)I Partner

S4.3.1 Voriconazole

Table S11: Drug-dependent parameters of the voriconazole PBPK model [52]

Parameter	Unit	Value	Source	Description
Voriconazole				
Molecular weight	g/mol	349.30	Lit.	Molecular weight
pKa, base		1.60	Lit.	Acid dissociation constant
Solubility (pH)	mg/L	3.20 (1.00), 2.70 (1.20), 0.10 (7.00)	Lit.	Solubility
Lipophilicity		1.80	Lit.	Lipophilicity
f_u	%	42.00	Lit.	Fraction unbound
CYP2C19 $K_M \rightarrow$ sink	$\mu\text{mol/L}$	3.50	Lit.	Michaelis-Menten constant
CYP2C19 $k_{\text{cat}} \rightarrow$ sink	1/min	1.19	Lit.	Catalytic rate constant
CYP3A4 $K_M \rightarrow$ sink	$\mu\text{mol/L}$	15.00	Lit.	Michaelis-Menten constant
CYP3A4 $k_{\text{cat}} \rightarrow$ sink	1/min	2.12	Opt.	Transport rate constant
GFR fraction		1 ^a	Asm.	Filtered drug in the urine
EHC continuous fraction		1	Asm.	Bile fraction continuously released
Intestinal permeability	cm/s	$2.71 \cdot 10^{-4}$	Opt.	Transcellular intestinal permeability
Cellular permeability	cm/min	PK-Sim Standard, $2.58 \cdot 10^{-3}$	Calc. [47]	Permeability into the cellular space
Partition coefficients		Poulin and Theil	Calc. [53–56]	Organ-plasma partition coefficients
Dissolution time (Weibull)	min	30.00	Opt.	Dissolution time (50%)
Dissolution shape (Weibull)		1.29	Opt.	Dissolution shape
CYP2C19 K_i	$\mu\text{mol/L}$	4.57	Lit.	Diss. const. inhibitor-enzyme complex (CI)
CYP3A4 K_i	$\mu\text{mol/L}$	9.33	Meas.	Conc. for half-maximal inactivation (MBI)
CYP3A4 k_{inact}	1/min	0.02	Opt.	Maximum inactivation rate constant (MBI)
CYP3A5 K_i	$\mu\text{mol/L}$	0.20 ^b	Lit. [57]	Diss. const. inhibitor-enzyme complex (CI)

^a: a GFR fraction of 1 corresponds to passive glomerular filtration of a compound, ^b: added to the original model, asm.: assumed, calc.: calculated, CI: competitive inhibition, conc.: concentration, const.: constant, CYP: cytochrome P450, diss.: dissociation, EHC: enterohepatic circulation, GFR: glomerular filtration rate, lit.: literature, meas.: measured, opt.: optimized. CYP2C19 drug-gene interactions were modeled by adjusting the reference concentration in the tissue of highest expression, i.e., for normal metabolizers 0.76 $\mu\text{mol protein/L}$ was implemented, for intermediate metabolizers 0.4 $\mu\text{mol protein/L}$, and for poor metabolizers 0.01 $\mu\text{mol protein/L}$.

S4.3.2 Itraconazole

Table S12: Drug-dependent parameters of the itraconazole PBPK model [7]

Parameter	Unit	Value	Source	Description
Itraconazole				
Molecular weight	g/mol	705.63	Lit.	Molecular weight
pKa, base		3.70	Lit.	Acid dissociation constant
Solubility (pH)	mg/L	8.00 (6.50)	Lit.	Solubility
Lipophilicity		4.62	Opt.	Lipophilicity
f_u	%	0.60	Lit.	Fraction unbound
CYP3A4 $K_M \rightarrow$ OH-Itra	nmol/L	2.07	Lit.	Michaelis-Menten constant
CYP3A4 $k_{cat} \rightarrow$ OH-Itra	1/min	0.04	Opt.	Transport rate constant
GFR fraction		1 ^a	Asm.	Filtered drug in the urine
EHC continuous fraction		1	Asm.	Bile fraction continuously released
Intestinal permeability	dm/min	$5.33 \cdot 10^{-5}$	Opt.	Transcellular intestinal permeability
Cellular permeability	cm/min	PK-Sim Standard, 0.01	Calc. [47]	Permeability into the cellular space
Partition coefficients		Rodgers + Rowland	Calc. [58, 59]	Organ-plasma partition coefficients
Dissolution time (Weibull)	min	406.30	Opt.	Dissolution time (50%)
Dissolution shape (Weibull)		1.43	Opt.	Dissolution shape
CYP3A4 K_i	nmol/L	1.30	Lit.	Diss. const. inhibitor-enzyme complex (CI)
CYP3A5 K_i	μ mol/L	0.94 ^b	Lit. [57]	Diss. const. inhibitor-enzyme complex (CI)
Hydroxy-Itraconazole				
Molecular weight	g/mol	721.63	Lit.	Molecular weight
pKa, base		3.70	Lit.	Acid dissociation constant

^a: a GFR fraction of 1 corresponds to passive glomerular filtration of a compound, ^b: added to the original model, asm.: assumed, calc.: calculated, CI: competitive inhibition, conc.: concentration, const.: constant, CYP: cytochrome P450, diss.: dissociation, EHC: entero-hepatic circulation, GFR: glomerular filtration rate, Keto-Itra: keto-itraconazole, lit.: literature, N-Des-Itra: N-desalkyl-itraconazole, OH-Itra: hydroxy-itraconazole, opt.: optimized.

Table S12: Drug-dependent parameters of the itraconazole PBPK model [7] (*continued*)

Parameter	Unit	Value	Source	Description
Solubility (pH)	mg/L	1.00 (7.00)	Asm.	Solubility
Lipophilicity		3.72	Opt.	Lipophilicity
f_u	%	1.70	Lit.	Fraction unbound
CYP3A4 $K_M \rightarrow$ Keto-Itra	nmol/L	4.17	Lit.	Michaelis-Menten constant
CYP3A4 $k_{cat} \rightarrow$ Keto-Itra	1/min	0.02	Opt.	Transport rate constant
GFR fraction		1 ^a	Asm.	Filtered drug in the urine
EHC continuous fraction		1	Asm.	Bile fraction continuously released
Intestinal permeability	cm/min	$1.52 \cdot 10^{-5}$	Calc.	Transcellular intestinal permeability
Cellular permeability	cm/min	PK-Sim Standard, $1.55 \cdot 10^{-3}$	Calc. [47]	Permeability into the cellular space
Partition coefficients		Rodgers + Roland	Calc. [58, 59]	Organ-plasma partition coefficients
CYP3A4 K_i	nmol/L	14.40	Lit.	Diss. const. inhibitor-enzyme complex (CI)
Keto-Itraconazole				
Molecular weight	g/mol	719.62	Lit.	Molecular weight
pKa, base		3.70	Lit.	Acid dissociation constant
Solubility (pH)	mg/L	1.00 (7.00)	Asm.	Solubility
Lipophilicity		4.21	Opt.	Lipophilicity
f_u	%	1.00	Lit.	Fraction unbound
CYP3A4 $K_M \rightarrow$ N-Des-Itra	nmol/L	2.22	Lit.	Michaelis-Menten constant
CYP3A4 $k_{cat} \rightarrow$ N-Des-Itra	1/min	0.39	Opt.	Transport rate constant
GFR fraction		1 ^a	Asm.	Filtered drug in the urine
EHC continuous fraction		1	Asm.	Bile fraction continuously released
Intestinal permeability	cm/min	$4.79 \cdot 10^{-5}$	Calc.	Transcellular intestinal permeability
Cellular permeability	cm/min	PK-Sim Standard, $4.92 \cdot 10^{-3}$	Calc. [47]	Permeability into the cellular space
Partition coefficients		Rodgers + Roland	Calc. [58, 59]	Organ-plasma partition coefficients
CYP3A4 K_i	nmol/L	5.12	Lit.	Diss. const. inhibitor-enzyme complex (CI)

^a: a GFR fraction of 1 corresponds to passive glomerular filtration of a compound, ^b: added to the original model, asm.: assumed, calc.: calculated, CI: competitive inhibition, conc.: concentration, const.: constant, CYP: cytochrome P450, diss.: dissociation, EHC: entero-hepatic circulation, GFR: glomerular filtration rate, Keto-Itra: keto-itraconazole, lit.: literature, N-Des-Itra: N-desalkyl-itraconazole, OH-Itra: hydroxy-itraconazole, opt.: optimized.

Table S12: Drug-dependent parameters of the itraconazole PBPK model [7] (*continued*)

Parameter	Unit	Value	Source	Description
N-Desalkyl-Itraconazole				
Molecular weight	g/mol	649.53	Lit.	Molecular weight
pKa, base		3.70	Lit.	Acid dissociation constant
Solubility (pH)	mg/L	1.00 (7.00)	Asm.	Solubility
Lipophilicity		5.18	Opt.	Lipophilicity
f_u	%	1.10	Lit.	Fraction unbound
CYP3A4 $K_M \rightarrow$ sink	nmol/L	0.63	Lit.	Michaelis-Menten constant
CYP3A4 $k_{cat} \rightarrow$ sink	1/min	0.06	Opt.	Transport rate constant
GFR fraction		1 ^a	Asm.	Filtered drug in the urine
EHC continuous fraction		1	Asm.	Bile fraction continuously released
Intestinal permeability	cm/min	$7.37 \cdot 10^{-4}$	Calc.	Transcellular intestinal permeability
Cellular permeability	cm/min	PK-Sim Standard, 0.09	Calc. [47]	Permeability into the cellular space
Partition coefficients		Rodgers + Roland	Calc. [58, 59]	Organ-plasma partition coefficients
CYP3A4 K_i	nmol/L	0.32	Lit.	Diss. const. inhibitor-enzyme complex (CI)

^a: a GFR fraction of 1 corresponds to passive glomerular filtration of a compound, ^b: added to the original model, asm.: assumed, calc.: calculated, CI: competitive inhibition, conc.: concentration, const.: constant, CYP: cytochrome P450, diss.: dissociation, EHC: entero-hepatic circulation, GFR: glomerular filtration rate, Keto-Itra: keto-itraconazole, lit.: literature, N-Des-Itra: N-desalkyl-itraconazole, OH-Itra: hydroxy-itraconazole, opt.: optimized.

S4.3.3 Rifampicin

Table S13: Drug-dependent parameters of the rifampicin PBPK model [7]

Parameter	Unit	Value	Source	Description
Rifampicin				
Molecular weight	g/mol	822.94	Lit.	Molecular weight
pKa, base		7.90	Lit.	Acid dissociation constant
pKa, acid		1.70	Lit.	Acid dissociation constant
Solubility (pH)	mg/L	2800.00 (7.5)	Lit.	Solubility
Lipophilicity		2.50	Opt.	Lipophilicity
f_u	%	17.00	Lit.	Fraction unbound
AADAC $K_M \rightarrow$ sink	$\mu\text{mol/L}$	195.10	Lit.	Michaelis-Menten constant
AADAC $k_{\text{cat}} \rightarrow$ sink	1/min	9.87	Opt.	Catalytic rate constant
OATP1B1 K_M	$\mu\text{mol/L}$	1.50	Lit.	Michaelis-Menten constant
OATP1B1 k_{cat}	1/min	74.43 ^a	Opt.	Transport rate constant
P-gp K_M	$\mu\text{mol/L}$	55.00	Lit.	Michaelis-Menten constant
P-gp k_{cat}	1/min	0.61	Opt.	Transport rate constant
GFR fraction		1 ^b	Asm.	Filtered drug in the urine
EHC continuous fraction		1	Asm.	Bile fraction continuously released
Intestinal permeability	cm/min	$1.24 \cdot 10^{-5}$	Opt.	Transcellular intestinal permeability
Cellular permeability	cm/min	PK-Sim Standard, $2.93 \cdot 10^{-5}$	Calc. [47]	Permeability into the cellular space
Partition coefficients		Rodgers + Rowland	Calc. [58, 59]	Organ-plasma partition coefficients
Formulation		Solution		Formulation used in predictions

^a: adjusted due to different reference concentrations in the original model and tacrolimus model, ^b: a GFR fraction of 1 corresponds to passive glomerular filtration of a compound, AADAC: arylacetamide deacetylase, asm.: assumed, calc.: calculated, CI: competitive inhibition, conc.: concentration, const.: constant, CYP: cytochrome P450, diss.: dissociation, EHC: enterohepatic circulation, GFR: glomerular filtration rate, lit.: literature, OATP: organic-anion-transporting polypeptide, opt.: optimized, P-gp: P-glycoprotein.

Table S13: Drug-dependent parameters of the rifampicin PBPK model [7] (*continued*)

Parameter	Unit	Value	Source	Description
Induction EC_{50}	$\mu\text{mol/L}$	0.34	Lit.	Conc. for half-maximal induction
AADAC E_{max}		0.99	Opt.	Maximum induction effect
CYP3A4 E_{max}		9.00	Lit.	Maximum induction effect
CYP3A4 K_i	$\mu\text{mol/L}$	18.50	Lit.	Diss. const. inhibitor-enzyme complex (CI)
OATP1B1 E_{max}		0.38	Opt.	Maximum induction effect
OATP1B1 K_i	$\mu\text{mol/L}$	0.48	Lit.	Diss. const. inhibitor-enzyme complex (CI)
P-gp E_{max}		2.50	Lit.	Maximum induction effect
P-gp K_i	$\mu\text{mol/L}$	169.00	Lit.	Diss. const. inhibitor-enzyme complex (CI)

^a: adjusted due to different reference concentrations in the original model and tacrolimus model, ^b: a GFR fraction of 1 corresponds to passive glomerular filtration of a compound, AADAC: arylacetamide deacetylase, asm.: assumed, calc.: calculated, CI: competitive inhibition, conc.: concentration, const.: constant, CYP: cytochrome P450, diss.: dissociation, EHC: enterohepatic circulation, GFR: glomerular filtration rate, lit.: literature, OATP: organic-anion-transporting polypeptide, opt.: optimized, P-gp: P-glycoprotein.

S4.4 Whole Blood Concentration-Time Profiles (Semilogarithmic)

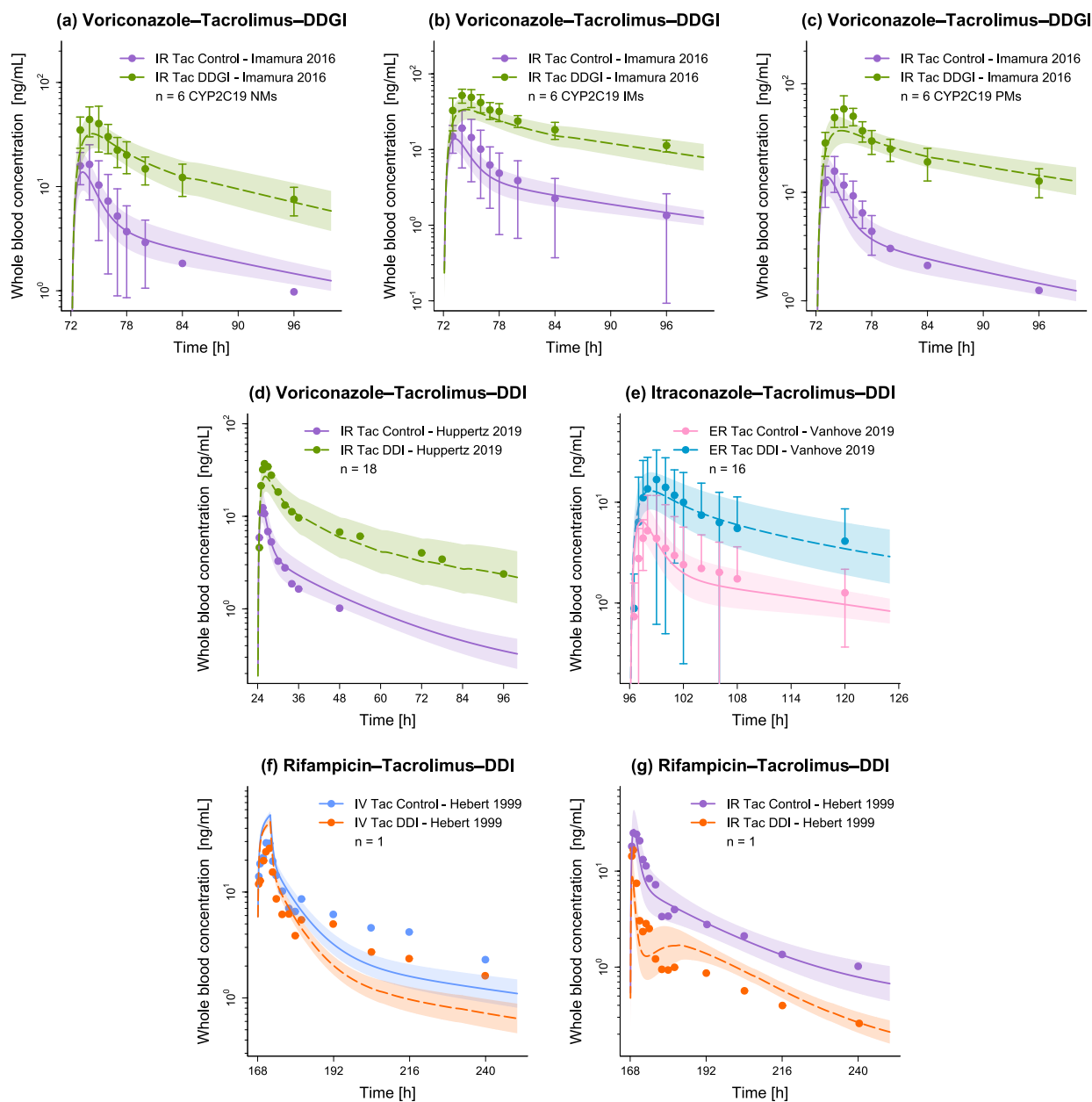


Figure S20: Evaluation of the modeled drug-drug(-gene) interactions. Presented are predicted whole blood concentration-time profiles (semilogarithmic plots) of tacrolimus without (Control) and with (DD(G)I) intake of the respective perpetrator drug (voriconazole (a–d), itraconazole (e), rifampicin (f–g)), alongside corresponding observed data [31, 49–51]. Solid (Control) and dashed (DD(G)I) lines and ribbons represent population predictions ($n = 1000$; geometric mean and geometric standard deviation), while corresponding observed data are shown as dots (\pm standard deviation, if available). CYP: cytochrome P450, DD(G)I: drug-drug(-gene) interaction, ER: extended-release, IM: intermediate metabolizer, IR: immediate-release, IV: intravenous, n : number of participants, NM: normal metabolizer, PM: poor metabolizer, Tac: tacrolimus.

S4.5 Whole Blood Concentration-Time Profiles (Linear)

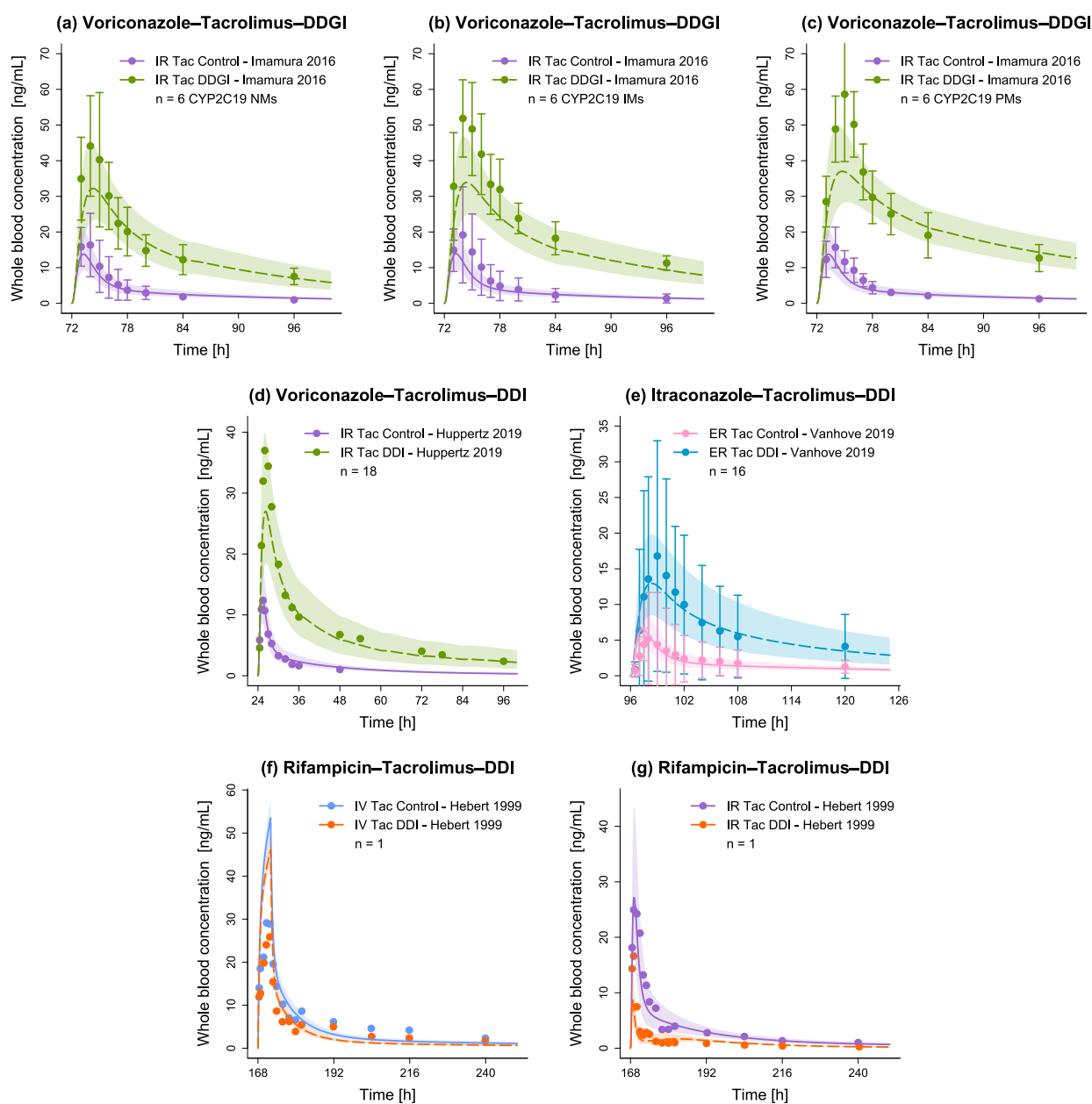


Figure S21: Evaluation of the modeled drug-drug(-gene) interactions. Presented are predicted whole blood concentration-time profiles (linear plots) of tacrolimus without (Control) and with (DD(G)I) intake of the respective perpetrator drug (voriconazole (a–d), itraconazole (e), rifampicin (f–g)), alongside corresponding observed data [31, 49–51]. Solid (Control) and dashed (DD(G)I) lines and ribbons represent population predictions ($n = 1000$; geometric mean and geometric standard deviation), while corresponding observed data are shown as dots (\pm standard deviation, if available). CYP: cytochrome P450, DD(G)I: drug-drug(-gene) interaction, ER: extended-release, IM: intermediate metabolizer, IR: immediate-release, IV: intravenous, n: number of participants, NM: normal metabolizer, PM: poor metabolizer, Tac: tacrolimus.

S4.6 DD(G)I AUC_{last} and DD(G)I C_{max} Ratio Goodness-of-Fit Plots

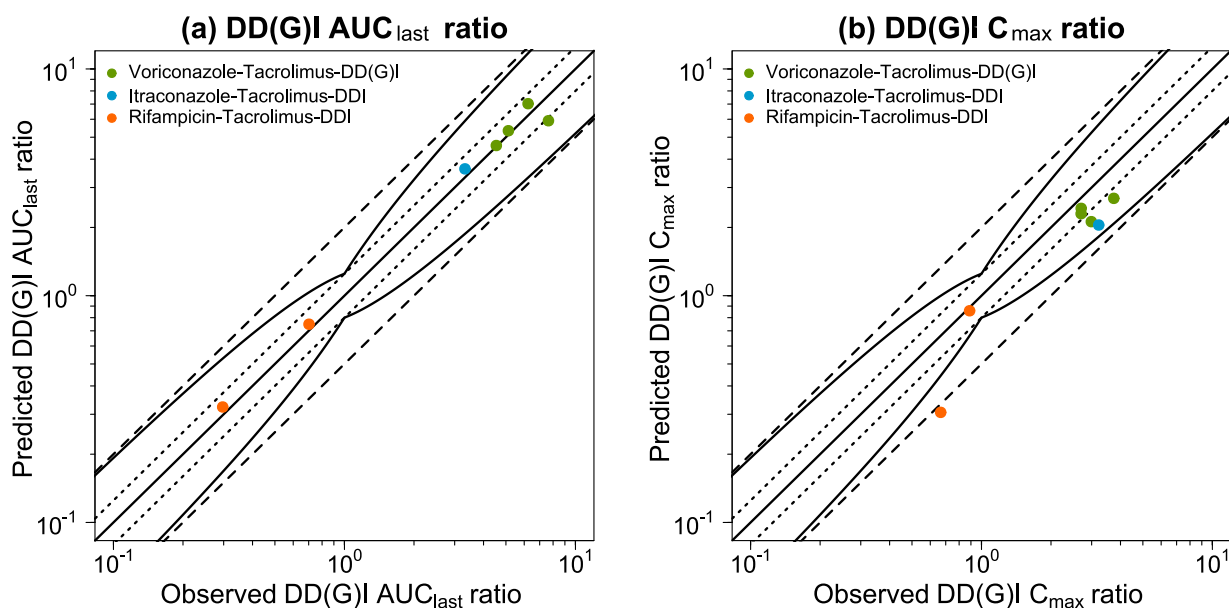


Figure S22: Evaluation of the modeled drug-drug(-gene) interactions. Predicted versus observed DD(G)I AUC_{last} (a) and DD(G)I C_{max} (b) ratios are shown with the solid line representing the line of identity, dotted lines indicating 1.25-fold and dashed lines 2-fold deviation from the respective observed value, along with the curved lines marking the prediction success limits proposed by Guest et al.[46] including 20% variability. AUC_{last} : area under the whole blood concentration-time curve determined between first and last concentration measurements, C_{max} : maximum whole blood concentration, DD(G)I: drug-drug(-gene) interaction.

S4.7 Predicted and Observed DD(G)I AUC_{last} and DD(G)I C_{max} Ratios

Table S14: Predicted versus observed DD(G)I AUC_{last} and DD(G)I C_{max} ratios

Tacrolimus application [mg]	Perpetrator	Perpetrator application [mg]	n	DD(G)I AUC _{last} ratio			DD(G)I C _{max} ratio			Reference
				Pred	Obs	Pred/Obs	Pred	Obs	Pred/Obs	
d4: 3 po (IR cap, SD)	Voriconazole	d1: 400, d2–4: 200 po (tab, BID)	6 NM CYP2C19	4.60	4.54	1.01	2.30	2.70	0.85	Imamura 2016 [49]
d4: 3 po (IR cap, SD)	Voriconazole	d1: 400, d2–4: 200 po (tab, BID)	6 IM CYP2C19	5.34	5.12	1.04	2.43	2.70	0.90	Imamura 2016 [49]
d4: 3 po (IR cap, SD)	Voriconazole	d1: 400, d2–4: 200 po (tab, BID)	6 PM CYP2C19	7.03	6.23	1.13	2.69	3.74	0.72	Imamura 2016 [49]
d2: 3 po (IR cap, SD)	Voriconazole ^a	d1: 400, d2–4: 200 po (tab, BID)	18	5.90	7.64	0.77	2.12	2.99	0.71	Huppertz 2019 [50]
d5: 3 po (ER cap, SD)	Itraconazole ^b	d1–4: 200 po (cap, BID)	16	3.63	3.32	1.09	2.05	3.22	0.64	Vanhove 2019 [31]
d8: 0.025/kg iv (inf, 4 h, SD)	Rifampicin	d1–18: 600 po (cap, MD)	1	0.75	0.70	1.07	0.86	0.89	0.97	Hebert 1999 [51]
d8: 8 po (IR cap, SD)	Rifampicin	d1–18: 600 po (cap, MD)	1	0.32	0.30	1.09	0.31	0.67	0.46	Hebert 1999 [51]
Overall mean GMFE (range) GMFE ≤ 2				1.10 (1.01–1.29) 7/7			1.41 (1.04–2.18) 6/7			

^a: plus midazolam (not included in the model): d2; 0.03 mg; po (solution, SD), ^b: plus midazolam (not included in the model): d5; 2 mg; po (solution, SD), AUC_{last}: area under the whole blood concentration-time curve determined between first and last concentration measurements, BID: multiple dose (twice daily), cap: capsule, C_{max}: maximum whole blood concentration, CYP: cytochrome P450, d: day, DD(G)I: drug-drug(-gene) interaction, ER: extended-release, IM: intermediate metabolizer, inf: infusion, iv: intravenous, GMFE: geometric mean fold error, IR: immediate-release, MD: multiple dose (once daily), n: number of participants, NM: normal metabolizer, PM: poor metabolizer, po: oral, pred: predicted, SD: single dose, tab: tablet.

Bibliography

- [1] M Nishimura and S Naito. Tissue-specific mRNA expression profiles of human phase I metabolizing enzymes except for cytochrome P450 and phase II metabolizing enzymes. *Drug metabolism and pharmacokinetics*, 21(5):357–374, 2006.
- [2] AD Rodrigues. Integrated cytochrome P450 reaction phenotyping. Attempting to bridge the gap between cDNA-expressed cytochromes P450 and native human liver microsomes. *Biochemical Pharmacology*, 57(5):465–480, 1999.
- [3] Open Systems Pharmacology Suite Community PK-Sim®Ontogeny Database Documentation, Available online (accessed on 30 April 2022). URL <https://github.com/Open-Systems-Pharmacology/OSPSuite.Documentation/blob/master/PK-SimOntogenyDatabaseVersion7.3.pdf>.
- [4] M Nishimura, H Yaguti, H Yoshitsugu, and S Naito. Tissue distribution of mRNA expression of human cytochrome P450 isoforms assessed by high-sensitivity real-time reverse transcription PCR. *Journal of the Pharmaceutical Society of Japan*, 123(5):369 – 375, 2003.
- [5] B Prasad, R Evers, A Gupta, CECA Hop, L Salphati, S Shukla, S Ambudkar, and JD Unadkat. Interindividual variability in hepatic OATPs and P-glycoprotein (ABCB1) protein expression: Quantification by LC-MS/MS and influence of genotype, age and sex. *Drug metabolism and disposition: the biological fate of chemicals*, 42(1):78–88, 2014.
- [6] M Nishimura and S Naito. Tissue-specific mRNA expression profiles of human ATP-binding cassette and solute carrier transporter superfamilies. *Drug metabolism and pharmacokinetics*, 20(6):452–477, 2005.
- [7] N Hanke, S Frechen, D Moj, H Britz, T Eissing, T Wendl, and T Lehr. PBPK models for CYP3A4 and P-gp DDI prediction: A modeling network of rifampicin, itraconazole, clarithromycin, midazolam, alfentanil, and digoxin. *CPT: Pharmacometrics and Systems Pharmacology*, 7(10):647–659, oct 2018.
- [8] M Meyer, S Schneckener, B Ludewig, L Kuepfer, and J Lippert. Using expression data for quantification of active processes in physiologically based pharmacokinetic modeling. *Drug metabolism and disposition: the biological fate of chemicals*, 40(5):892–901, may 2012.
- [9] LM Mancinelli, L Frassetto, LC Floren, D Dressler, S Carrier, I Bekersky, LZ Benet, and U Christians. The pharmacokinetics and metabolic disposition of tacrolimus: A comparison across ethnic groups. *Clinical Pharmacology and Therapeutics*, 69(1):24–31, 2001.
- [10] I Bekersky, D Dressler, A Alak, GW Boswell, and QA Mekki. Comparative tacrolimus pharmacokinetics: Normal versus mildly hepatically impaired subjects. *Journal of Clinical Pharmacology*, 41(6):628–635, 2001.
- [11] LC Floren, I Bekersky, LZ Benet, QA Mekki, D Dressier, JW Lee, JP Roberts, and MF Hebert. Tacrolimus oral bioavailability doubles with coadministration of ketoconazole. *Clinical Pharmacology and Therapeutics*, 62(1):41–49, 1997.
- [12] P Mathew, J Mandal, K Patel, K Soni, G Tangudu, R Patel, and P Kale. Bioequivalence of two tacrolimus formulations under fasting conditions in healthy male subjects. *Clinical Therapeutics*, 33(9):1105–1119, 2011.
- [13] YK Kim, A Kim, SJ Park, and H Lee. New tablet formulation of tacrolimus with smaller interindividual variability may become a better treatment option than the conventional capsule formulation in organ transplant patients. *Drug Design, Development and Therapy*, 11:2861–2869, 2017.

- [14] S Wring, G Murphy, G Atiee, C Corr, M Hyman, M Willett, and D Angulo. Clinical pharmacokinetics and drug-drug interaction potential for coadministered SCY-078, an oral fungicidal glucan synthase inhibitor, and tacrolimus. *Clinical Pharmacology in Drug Development*, 8(1): 60–69, 2019.
- [15] F Itagaki, M Homma, K Yuzawa, M Nishimura, S Naito, N Ueda, N Ohkohchi, and Y Kohda. Effect of lansoprazole and rabeprazole on tacrolimus pharmacokinetics in healthy volunteers with CYP2C19 mutations. *Journal of Pharmacy and Pharmacology*, 56(8):1055–1059, 2004.
- [16] I Bekersky, D Dressler, and QA Mekki. Dose linearity after oral administration of tacrolimus 1-mg capsules at doses of 3, 7, and 10 mg. *Clinical Therapeutics*, 21(12):2058–2064, 1999.
- [17] I Bekersky, D Dressler, GW Boswell, B Fergen, W Tracewell, and QA Mekki. Bioequivalence of a new strength tacrolimus capsule under development. *Transplantation Proceedings*, 30(4): 1457–1459, 1998.
- [18] A Sansone-Parsons, G Krishna, M Martinho, B Kantalaria, S Gelone, and TG Mant. Effect of oral posaconazole on the pharmacokinetics of cyclosporine and tacrolimus. *Pharmacotherapy*, 27(6):825–834, 2007.
- [19] S Zheng, Y Tasnif, MF Hebert, CL Davis, Y Shitara, JC Calamia, YS Lin, DD Shen, and KE Thummel. Measurement and compartmental modeling of the effect of CYP3A5 gene variation on systemic and intrarenal tacrolimus disposition. *Clinical Pharmacology and Therapeutics*, 92(6):737–745, 2012.
- [20] I Bekersky, D Dressler, W Colburn, and QA Mekki. Bioequivalence of 1 and 5 mg tacrolimus capsules using a replicate study design. *Journal of Clinical Pharmacology*, 39(10):1032–1037, 1999.
- [21] A Lainesse, S Hussain, T Monif, S Reyar, SK Tippabhotla, A Madan, and NR Thudi. Bioequivalence studies of tacrolimus capsule under fasting and fed conditions in healthy male and female subjects. *Arzneimittel-Forschung/Drug Research*, 58(5):242–247, 2008.
- [22] I Bekersky, D Dressler, and QA Mekki. Effect of low- and high-fat meals on tacrolimus absorption following 5 mg single oral doses to healthy human subjects. *Journal of Clinical Pharmacology*, 41(2):176–182, 2001.
- [23] AH Groll, A Desai, D Han, C Howieson, K Kato, S Akhtar, D Kowalski, C Lademacher, W Lewis, H Pearlman, D Mandarino, T Yamazaki, and R Townsend. Pharmacokinetic assessment of drug-drug interactions of isavuconazole with the immunosuppressants cyclosporine, mycophenolic acid, prednisolone, sirolimus, and tacrolimus in healthy adults. *Clinical Pharmacology in Drug Development*, 6(1):76–85, 2017.
- [24] A Huppertz, J Bollmann, R Behnisch, T Bruckner, M Zorn, J Burhenne, WE Haefeli, and D Czock. Differential effect of a continental breakfast on tacrolimus formulations with different release characteristics. *Clinical Pharmacology in Drug Development*, 10(8):899–907, 2021.
- [25] JA Dowell, M Stogniew, D Krause, T Henkel, and B Damle. Lack of pharmacokinetic interaction between anidulafungin and tacrolimus. *Journal of Clinical Pharmacology*, 47(3):305–314, 2007.
- [26] I Bekersky, D Dressler, and QA Mekki. Effect of time of meal consumption on bioavailability of a single oral 5 mg tacrolimus dose. *Journal of Clinical Pharmacology*, 41(3):289–297, 2001.
- [27] RR Alloway, J Trofe-Clark, DC Brennan, J Kerr, EA Cohen, U Meier-Kriesche, DR Stevens, MA Moten, and JD Momper. Chronopharmacokinetics and food effects of single-dose LCP-tacrolimus in healthy volunteers. *Therapeutic drug monitoring*, 42(5):679–685, 2020.

- [28] F Stiff, F Vanmolokot, I Scheffers, L Van Bortel, C Neef, and M Christiaans. Rectal and sublingual administration of tacrolimus: A single-dose pharmacokinetic study in healthy volunteers. *British Journal of Clinical Pharmacology*, 78(5):996–1004, 2014.
- [29] MA Tortorici, V Parks, K Matschke, J Korth-Bradley, and A Patat. The evaluation of potential pharmacokinetic interaction between sirolimus and tacrolimus in healthy volunteers. *European Journal of Clinical Pharmacology*, 69(4):835–842, 2013.
- [30] A Mercuri, S Wu, S Stranzinger, S Mohr, S Salar-Behzadi, M Bresciani, and E Fröhlich. In vitro and in silico characterisation of tacrolimus released under biorelevant conditions. *International Journal of Pharmaceutics*, 515(1-2):271–280, 2016.
- [31] T Vanhove, P Annaert, N Knops, H de Loor, J de Hoon, and DRJ Kuypers. In vivo CYP3A4 activity does not predict the magnitude of interaction between itraconazole and tacrolimus from an extended release formulation. *Basic and Clinical Pharmacology and Toxicology*, 124(1):50–55, 2019.
- [32] K Gantar, K Škerget, I Mochkin, and A Bajc. Meeting regulatory requirements for drugs with a narrow therapeutic index: Bioequivalence studies of generic once-daily tacrolimus. *Drug, Healthcare and Patient Safety*, 12:151–160, 2020.
- [33] N Undre and J Dickinson. Relative bioavailability of single doses of prolonged-release tacrolimus administered as a suspension, orally or via a nasogastric tube, compared with intact capsules: A phase 1 study in healthy participants. *BMJ Open*, 7(4):1–7, 2017.
- [34] RP Austin, P Barton, SL Cockroft, MC Wenlock, and RJ Riley. The influence of nonspecific microsomal binding on apparent intrinsic clearance, and its prediction from physicochemical properties. *Drug Metabolism and Disposition*, 30(12):1497–1503, 2002.
- [35] F Langenbucher. Linearization of dissolution rate by the Weibull distribution. *J Pharm Pharmacol*, 24(12):979–981, 1972.
- [36] ChemAxon Tacrolimus, Available online (accessed on 23 April 2022). URL <https://chemicalize.com/app/calculation>.
- [37] AI Lauerma, C Surber, and HI Maibach. Absorption of topical tacrolimus (FK506) in vitro through human skin: Comparison with cyclosporin A. *Skin Pharmacology and Physiology*, 10(5-6):230–234, 1997.
- [38] SE Lucangioli, E Kenndler, A Carlucci, VP Tripodi, SL Scioscia, and CN Carducci. Relation between retention factors of immunosuppressive drugs in microemulsion electrokinetic chromatography with biosurfactants and octanol-water partition coefficients. *Journal of Pharmaceutical and Biomedical Analysis*, 33(5):871–878, 2003.
- [39] H Zahir, RA Nand, KF Brown, BN Tattam, and AJ McLachlan. Validation of methods to study the distribution and protein binding of tacrolimus in human blood. *Journal of Pharmacological and Toxicological Methods*, 46(1):27–35, 2001.
- [40] Y Dai, MF Hebert, N Isoherranen, CL Davis, C Marsh, DD Shen, and KE Thummel. Effect of CYP3A5 polymorphism on tacrolimus metabolic clearance in vitro. *Drug Metabolism and Disposition*, 34(5):836–847, 2006.
- [41] LK Kamdem, F Streit, UM Zanger, J Brockmüller, M Oellerich, VW Armstrong, and L Wojnowski. Contribution of CYP3A5 to the in vitro hepatic clearance of tacrolimus. *Clinical Chemistry*, 51(8):1374–1381, 2005.
- [42] R Kawai, M Lemaire, JL Steimer, A Bruelisauer, W Niederberger, and M Rowland. Physiologically based pharmacokinetic study on a cyclosporin derivative, SDZ IMM 125. *Journal of Pharmacokinetics and Biopharmaceutics*, 22(5):327–365, 1994.

- [43] LM Berezhkovskiy. Volume of distribution at steady state for a linear pharmacokinetic system with peripheral elimination. *Journal of Pharmaceutical Sciences*, 93(6):1628–40, 2004.
- [44] JA Petan, N Undre, MR First, K Saito, T Ohara, O Iwabe, H Mimura, M Suzuki, and S Kitamura. Physicochemical properties of generic formulations of tacrolimus in Mexico. *Transplantation Proceedings*, 40(5):1439–1442, 2008.
- [45] R Amundsen, A Åsberg, IK Ohm, and H Christensen. Cyclosporine A- and tacrolimus-mediated inhibition of CYP3A4 and CYP3A5 in vitro. 40(4):655–661, 2012.
- [46] EJ Guest, L Aarons, JB Houston, A Rostami-Hodjegan, and A Galetin. Critique of the two-fold measure of prediction success for ratios: Application for the assessment of drug-drug interactions. *Drug Metabolism and Disposition*, 39(2):170–173, 2011.
- [47] Open Systems Pharmacology Suite Community. Open Systems Pharmacology Suite Manual, Version 7.4 2018, Available online (accessed on 28 September 2021). URL <https://docs.open-systems-pharmacology.org/working-with-pk-sim/pk-sim-documentation>.
- [48] JH Lin. CYP induction-mediated drug interactions: In vitro assessment and clinical implications. *Pharmaceutical Research*, 23(6):1089–1116, 2006.
- [49] CK Imamura, K Furihata, S Okamoto, and Y Tanigawara. Impact of cytochrome P450 2C19 polymorphisms on the pharmacokinetics of tacrolimus when coadministered with voriconazole. *Journal of Clinical Pharmacology*, 56(4):408–413, 2016.
- [50] A Huppertz, C Ott, T Bruckner, KI Foerster, J Burhenne, J Weiss, M Zorn, WE Haefeli, and D Czock. Prolonged-release tacrolimus is less susceptible to interaction with the strong CYP3A inhibitor voriconazole in healthy volunteers. *Clinical Pharmacology and Therapeutics*, 106(6):1290–1298, 2019.
- [51] M F Hebert, R M Fisher, C L Marsh, D Dressler, and I Bekersky. Effects of rifampin on tacrolimus pharmacokinetics in healthy volunteers. *Journal of Clinical Pharmacology*, 39(1):91–96, 1999. doi: 10.1177/00912709922007499.
- [52] X Li, S Frechen, D Moj, T Lehr, M Taubert, CH Hsin, G Mikus, PJ Neuvonen, KT Olkkola, TI Saari, and U Fuhr. A physiologically based pharmacokinetic model of voriconazole integrating time-dependent inhibition of CYP3A4, genetic polymorphisms of CYP2C19 and predictions of drug-drug interactions. *Clinical Pharmacokinetics*, 59(6):781–808, 2020.
- [53] P Poulin, K Schoenlein, and PF Theil. Prediction of adipose tissue: plasma partition coefficients for structurally unrelated drugs. *Journal of pharmaceutical sciences*, 90(4):436–447, 2001.
- [54] P Poulin and FP Theil. A priori prediction of tissue:plasma partition coefficients of drugs to facilitate the use of physiologically-based pharmacokinetic models in drug discovery. *Journal of pharmaceutical sciences*, 89(1):16–35, 2000.
- [55] P Poulin and FP Theil. Prediction of pharmacokinetics prior to in vivo studies. 1. Mechanism-based prediction of volume of distribution. *Journal of pharmaceutical sciences*, 91(1):129–156, 2002.
- [56] P Poulin and FP Theil. Prediction of pharmacokinetics prior to in vivo studies. II. Generic physiologically based pharmacokinetic models of drug disposition. *Journal of pharmaceutical sciences*, 91(5):1358–1370, 2002.
- [57] H Yamazaki, M Nakamoto, M Shimizu, N Murayama, and T Niwa. Potential impact of cytochrome P450 3A5 in human liver on drug interactions with triazoles. *British Journal of Clinical Pharmacology*, 69(6):593–597, 2010.

- [58] T Rodgers, D Leahy, and M Rowland. Physiologically based pharmacokinetic modeling 1: predicting the tissue distribution of moderate-to-strong bases. *Journal of pharmaceutical sciences*, 94(6):1259–1276, 2005.
- [59] T Rodgers and M Rowland. Physiologically based pharmacokinetic modelling 2: predicting the tissue distribution of acids, very weak bases, neutrals and zwitterions. *Journal of pharmaceutical sciences*, 95(6):1238–1257, 2006.